論文 / 著書情報
Article / Book Information

Title	Triaxial erosion test for evaluation of mechanical consequences of internal erosion
Authors	Lin Ke, Akihiro Takahashi
Citation	Geotechnical Testing Journal, Vol. 37, No. 2, pp. 347-364
Pub. date	2014, 3
Copyright	This is a preprint of an article published in Geotechnical Testing Journal, (c) 2014, ASTM International, West Conshohocken, PA, http://dx.doi.org/10.1520/GTJ20130049, www.astm.org.

Triaxial erosion test for evaluation of mechanical consequences of internal erosion

Lin Ke and Akihiro Takahashi*

Lin Ke
Graduate student, Department of Civil Engineering,
Tokyo Institute of Technology, Japan
E-mail: ke.l.aa@m.titech.ac.jp

Akihiro Takahashi*
Associate Professor, Department of Civil Engineering
Tokyo Institute of Technology, Japan
E-mail: takihiro@cv.titech.ac.jp
* Corresponding author

Geotechnical Testing Journal 37 (2), 347-364, 2014

Official URL:

http://dx.doi.org/10.1520/GTJ20130049

1 Introduction

It is universally recognized that seepage-induced erosion would lead to catastrophic consequences: approximately half of the dam failures are due to soil erosion (Richards and Reddy, 2007). The phenomenon that those valleys on catchment topography, which may have been suffered from years of internal erosion, were vulnerable to fail during Noto Peninsula Earthquake of Japan in 2007 raises the concern about the possible influence of internal erosion on the soil microstructure change and, consequently, the strength change. The gap-graded soils, like sandy gravels or silty sands, are especially vulnerable to internal erosion because of their deficiency in certain grain size (Skempton and Brogan, 1994). Due to the inconformity of the definition of soil erosion in literature, the common term "internal erosion" is used here to describe the target phenomenon that small grains are eroded through the voids between the coarse grains by seepage flow. It develops chronically, usually accompanying with a great quantity of seepage flow over years. Meanwhile, during the internal erosion, there are dramatic changes in soil porosity and hydraulic conductivity. Muir Wood *et al.* (2010) proposed a theoretical model to evaluate the mechanical influence of internal erosion and concluded that the soil strength would decrease if significant amounts of fine grains were removed. Chang and Zhang (2011) experimentally proved this conclusion by a series of drained compression tests on the gap-graded cohesionless soil. It was found that the originally dilative soil would become contractive after internal erosion.

Although internal erosion is such a huge potential risk for the earth structure safety, hitherto, few laboratory tests have been fully developed to comprehensively assess the mechanical consequences of internal erosion on gap-graded sands by taking account of both monotonic and cyclic loadings. One of the main difficulties lies in guaranteeing a high saturation degree in soil specimens during erosion test, which can be hardly fulfilled in a conventional apparatus. Without a comparatively high saturation degree, laboratory tests on those internally eroded soils might not be well performed. Moreover, since internal erosion is chronic phenomenon, it would be better if the laboratory erosion tests could last for relatively long period. Upon those difficulties, this paper presents a newly developed triaxial seepage apparatus, capable of maintaining back pressure in a soil specimen during erosion test and directly obtaining the mechanical response of internally eroded soils. Preliminary test results, including drained monotonic tests, undrained monotonic tests and undrained cyclic tests on internally eroded soil, are discussed by comparing them with the mechanical responses of the specimens without erosion.

2 Critical Reviews of Available Internal Erosion Tests

The well-known standardized laboratory tests for soil erosion are pinhole test (ASTM D4647/D4647M-13) and the double hydrometer test (ASTM D4221-11), developed by Sherard *et al.* and Decker *et al.* respectively in the 1970s. The purpose of those tests is to identify the dispersive clay in soils, which are highly prone to internal erosion. The recently developed laboratory tests to study the soil erosion of cracks include slot erosion test (SET) and hole erosion test (HET) (Wan and Fell, 2004a and 2004b; Bonelli *et al.*, 2006; Haghighi *et al.*, 2013), which could determine the erosion rate, the minimum hydraulic shear stresses to initiate piping erosion, and their relationships to the soil properties. SET and HET are mainly served for the dam risk assessment. Indraratna *et al.* (2013) developed the Process Simulation Apparatus for Internal Crack Erosion (PSAICE) to assess the erosion rate of a sandy soil with cracks at different hydraulic gradients. For practical purpose, several other test methods have been proposed to evaluate the soil erosion potential in channels/canals or around the soil-structure surface, including flume test (Arulanandan and Peery, 1983), jet erosion test (Moore and Masch, 1962), rotating cylinder test (Moore and Masch, 1962) and erosion function test (Briaud *et al.*, 2001)

The phenomenon that the base soil that satisfies the geometrical criteria may fail due to erosion of fine grains, discovered in the base soil and filter compatibility studies inspired the laboratory test on those “poor graded” soils, such as gap-graded or coarse widely graded soils. In those experimental investigations, not only the soil geometric characteristics, but also the influence of flow velocity, flow direction, hydraulic gradient and possible chemical reaction is taken into consideration. The main apparatus comprises a permeameter cell together with the transducers for the measurement of pore water pressure spatial variations and effective stress distribution along the specimen. To prevent the formation of large seepage channels along the fixed-wall, an extra layer, such as a compressive rubber layer or a silicon grease layer against the inside wall is necessary. The permeameter cell is usually transparent in order to record the process of internal erosion by either microscopic or visual observation. For those cases conducted with external loading, the permeameter cell is mounted into a reaction frame to accommodate an axial loading system. Vertical effective stress on the top surface is calculated from axial force of the loading rod. A displacement transducer mounted on the loading rod monitors the axial displacement. The tested soils are either above one filter layer or sandwiched between two filter layers.

Controlled seepage flow is necessary for internal erosion test. Occasionally, a light vibration is also applied on soil sample to ensure full erosion. The seepage flow is usually unidirectional, either upward or downward, which is generated by the hydraulic pressure difference between the top and bottom of a specimen. In the earlier experiments, the inlet hydraulic pressure is maintained by a constant-water-head tank while the outlet is open to atmosphere or connected to another constant-water-head tank. The flow rate is estimated by measuring the volume of discharge effluent per minute by a cylinder. To overcome the possible errors in the constant head control system, several improvements have been applied. Tanaka and Toyokuni (1991) maintained the constant upstream water head by one stabilization tube and one overflow tube. Tomlinson and Vaid (2000) kept the hydraulic head at the inlet by throttling a valve open to the water supply pressure while that at the outlet is maintained by submerging the permeameter into a large water bath with a constant water head. Flow rate is monitored by the volume of effluent out of the water bath. The water circulation system is usually adopted in experiments as well. Lafleur (1984) recirculated the water by means of a system of solenoid valves that ensured refilling of the upstream tank when it was empty. Kenney and Lau (1985, 1986) pumped the water in the effluent tank back to upper water tank to fulfill the circulation of seepage water. However, those systems could not reach the comparatively high hydraulic gradient that is usually necessary to initiate internal erosion in soils subjected to surcharge. Two pressurized storage reservoirs, namely influent and effluent reservoirs, are introduced as inflow and outflow tank to obtain the larger hydraulic gradient. To prevent the dissolution of air into water, which might lead to great errors in erosion test, each tank has an internal membrane acting as an air-over-water interface. The water temperature in the storage reservoir and inlet/outlet tanks keeps at constant temperature (20±1°C).

The eroded soil collection system is of great significance for the internal erosion test. In case of non-cohesive soil, for the downward flow test, the eroded soil is collected at the base of a permeameter. A drainage system, such as a silicon hose directed by a conical trough, is better to be included to prevent the possible clogging. For upward flow test, a gentle air flow through a thin tube at the top of the sample could be applied to avoid the sedimentation of the eroded grains (Sterpi, 2003). With regard to those cases with difficulties in installing the soil collection system, especially for the upward flow test, a graphical method proposed by Kenney and Lau (1985) could be used to approximately assess the fraction of eroded fine grains as well as the largest eroded fine grains based on the amounts of movements of grain size distribution curves after erosion (Wan, 2006). In case of cohesive soil, a flow-through turbidimeter could be connected to the outlet pipe to assess the eroded soil mass (Bendahmane *et al.*, 2008; Marot *et al.*, 2011).

The weakness of the commonly used fixed-wall permeameters in the laboratory investigations is the sidewall leakage, which may result in great errors in calculating hydraulic conductivity. The flexible-wall permeameters, on the other hand, could minimize the leakage and permit applying back pressure to improve the saturation degree of tested specimens. By controlling the vertical and confining pressure, the vulnerability of soils to internal erosion could be tested under various stress states. Due to those merits, recent erosion tests are performed in a revised triaxial cell. Richards and Reddy (2010) developed a true triaxial piping test apparatus to assess the backwards erosion potential of a wide range of soils, particularly non-cohesive soils, at various stress states. The apparatus mainly consisted of the true triaxial load cell, capable of applying a range of mutually perpendicular pressures, inlet-outlet pressure control panel, an inlet-flow control panel, trubidimeter and several pressurized vessels. It is worth stressing that the key component of erosion triaxial test is the eroded soil collection system, the design of which should ensure the eroded soil grains are perfectly collected. Bendahmane *et al.* (2008) studied the influence of hydraulic and mechanical characteristics of cohesive soils on internal erosion in a developed triaxial apparatus. A drainage system was added at the bottom of the cell. The soil erosion rate was estimated through a photo sensor. Shwiyhat and Xiao (2010) studied the changes in soil hydraulic conductivity and soil volume induced by internal erosion. The base pedestal of the triaxial apparatus was modified to allow discharge effluent and eroded soil grains to be captured in an effluent tank. Similarly, Chang and Zhang (2011, 2013) investigated the internal erosion potential of gap-graded sands subjected to multi-step seepage flow and conducted drained compression test on those eroded sands. The eroded soil grains were collected by a detachable container at regular intervals.

The above-mentioned triaxial erosion tests are mostly hydraulic gradient controlled type. By imposing hydraulic pressure on a soil specimen, the internal erosion could initiate if the critical hydraulic gradient is reached. The inlet hydraulic pressure is usually maintained by a pressurized water tank and the outlet is open to the atmosphere. Under this circumstance, the test time is strictly restricted by the volume of the water tank. However, since internal erosion is a chronic phenomenon (it usually takes years in nature), a continuous constant seepage flow sustaining for a relatively long time is necessary. Another drawback with this setup is that back pressure could not be applied, which may result in a low saturation degree in tested specimens and consequently, a not well performed undrained compression test. The triaxial apparatus in this paper adopts the constant-flow-rate control mode, which would ensure continuous water supply for a relatively long time. Meanwhile, the back pressure is maintained on tested specimens during the erosion test through a specially designed buffer. Inside of the buffer, a consecutive monitoring system is installed which permits continuous recording of the eroded soil mass.

3 Triaxial Internal Erosion Apparatus

The newly developed triaxial internal erosion apparatus could directly investigate not only the hydraulic characteristics of soils at the onset and the progress of internal erosion but also the change of soil mechanical behaviors induced by internal erosion. It is applicable for testing non-cohesive soils. The design is improved after preliminary one-dimensional seepage tests in a fixed-wall permeameter (Ke and Takahashi, 2012). It mainly consists of a constant-flow-rate control unit, an automated triaxial system and eroded soil collection unit. The recorded variables include the pressure differences generated by the seepage flow, soil axial & radial strain, cumulative eroded soil mass and pore pressures. The whole system allows independently synchronous control of the hydraulic condition and the stress state of tested specimens. Photograph of the triaixial permeameter is shown in Fig. 1 and the schematic illustration of the overall system is shown in Fig. 2.

3.1 Constant-flow-rate control unit

Hydraulic gradient and Darcy velocity are the vital parameters for hydraulics. For those sands with large hydraulic conductivity (>0.001m/s), seepage test by the hydraulic-gradient-control manner may not be appropriate because of the comparatively small hydraulic gradient to intrigue and maintain the internal erosion. An accurate control of the hydraulic pressure and estimation of the head loss in tubes, valves and fittings is necessary, which however is difficult in practice. The flow-rate-control mode, on the other hand, could avoid the above-mentioned difficulties. Richard and Reddy (2010) concluded that flow velocity might be the fundamental characteristic responsible for erosion in non-cohesive materials, which could yield more consistent results. In this apparatus, the seepage test is performed by the constant-flow-rate manner. The control unit is composed of a rotary pump with the maximum flow rate of 1360mL/min for pumping water flow through the specimen and a Low Capacity Differential Pressure Transducer (LCDPT) for measuring the pressure drop from the top to the bottom of tested specimens. The output of LCDPT is highly linear within the range of 0~20kPa. In order to maintain the flow rate constant, all the flow channels are designed as the same size: 7.5mm-in-diameter plastic tubes with relatively large stiffness are used. To minimize the effect of tube stiffness on the measurement of deviator stress, the tube is arranged in spiral (Fig. 3). For common triaxial equipment, an annular porous stone is typically used at the interface between soil and water in the top cap. However, in this apparatus, instead of porous stone, a perforated plate is mounted in top cap, which directly attaches specimen, to minimize the possible water head loss. The same as is at the pedestal, the details of which will be given later. The seepage water is pumped from a water tank, which is filled with water and kept at room temperature, at least 24 hours before use. Since the back pressure is maintained during seepage tests, the volume of the indissolved air bubbles in seepage flow may be shrunk and their influence on the soil saturation degree may be minimized. During the experiment, the range of the assigned inflow rate must ensure the resulting pressure drop is well below the confining pressure to prevent the separation of membrane from soil specimen.

3.2 Automated triaxial system

The automated triaxial system used, capable of investigating either the static or cyclic soil behavior, could conduct measurements and controls by PC through 16-bit A/D and D/A converters. The vertical load could be automatically applied by a motor-gear system at any rate. The maximum load is 50kN. The system has zero backlash on reversal of the load, which would realize the continuous cyclic loading without any stress relaxation. The cell pressure is applied by the air pressure which is maintained constantly at 700kPa through an automatic air compressor. All the pressure lines are connected to a drying system to remove any condensed water. The control of the cell pressure is by E/P (Electronic to Pneumatic) transducers, which is linked to PC through a 16-bit D/A board. The axial load is measured by the load cell internally mounted above the top cap, which eliminates the effects of any friction on the loading shaft. The soil effective pressure is known from another Difference Pressure Transducer, which joins the specimen base and cell. Pore pressure is obtained at the base of a specimen by a pressure transducer mounted at the pedestal. Three pairs of clip gauges with the capacity of ±2mm are employed to measure the radial deformation. All the measuring devices are connected to amplifiers and then to a PC through a 16-bit A/D converter. All the controls of the triaxial testing and data recording are through a program with the interactive visual interface, written by Visual C++.

The base pedestal is specially designed to accommodate the internal erosion test (Fig. 4). The main component is the drainage system to prevent the possible accumulation of eroded soil at the bottom, which would cause clogging. It includes a conical trough and a plastic tube fitted at the outlet of the trough, directly connected to the soil collection system. This space gives freedom in determining the filter, either the granular type or the wire mesh with openings. A paradox comes up in the filter determination. For soil element test, it is significant to ease the influence of boundary frictions on the measured material properties. In practice, to minimize the non-uniformity in stresses and strains induced by end restraint, a lubrication layer, such as a silicone grease layer or latex rubber is utilized (Kuwano *et al.,* 2000). However, that layer would cause great water head loss and serious clogging during erosion test due to the high viscosity. A compromise in free ends may be necessary. In this apparatus, the filter is the 5mm-thick steel mesh with smooth surface (Fig. 5). The opening size of the mesh follows the recommendation of Japan Dam Conference which specified that the mesh should fully hold the coarse grains and permit the erosion of fines (Uno, 2009). The adopted opening size is 1mm in this apparatus.

3.3 Eroded soil collection unit

The main component of the eroded soil collection unit is the pressurized sedimentation tank (Fig. 6). The acrylic tube is mounted between a steel top and base plate, and is sealed by means of O-rings and five external tie rods. Inside of the tank, a 160mm-in-diameter acrylic cylinder with full of water is built in. During the seepage tests, the discharge effluent with dislodged fines directly flows into the cylinder through a pipe that connects the inlet valve and the cylinder. The end of the pipe is fully submerged in the cylinder to prevent the admission of air bubbles into the tested soil specimen. The cumulative eroded soil mass is gained by continuously weighing the light tray which is fully submerged in the cylinder to collect the eroded soil grains.

The waterproofed load cell that has high sensitivity could record the cumulative eroded soil weight within a continuous period. The theoretical resolution of the load cell is 0.00015N (approximately 0.015g). Due to the magnitude of noise and zero shift induced by the data collection system, some deviations may exist. To drain off the seepage water, a solenoid valve with timer is fixed at the outlet drainage line. The valve is capable of opening and closing at a determined interval of time. During erosion tests, the back pressure in the tested soil specimen is maintained through the sedimentation tank.

4 Main Testing Procedures

The purpose of the study is to investigate the erosion characteristics of the cohesionless soil and its mechanical consequences. Therefore, the main testing procedures include erosion tests on the reconstituted soil specimens, monotonic compression or cyclic shearing tests on the eroded specimens and post-erosion grain size distribution analysis. A detailed description of each procedure is presented as following:

4.1 Saturation and consolidation

The vacuum saturation procedure (ASTM D4767-11; JGS 0525-2000), including two stages, is adopted in this study. The top and bottom of the tested specimen is connected to two separate reservoirs. After specimen preparation, vacuum is supplied to the specimen through both water reservoirs gradually until -80kPa. The pressure difference between the specimen pressure and the cell pressure is kept constant as 20kPa during the increment of vacuum. Allow deaerated water slowly inject into the specimen upwardly. The inflow rate should be sufficiently slow to avoid the filtration of soil grains in the specimen. After three-quarters of the deaerated water has flowed through the specimen, slowly return the specimen pressure to 0kPa and increase the cell pressure to 20kPa, keeping the pressure increment constantly as 20kPa all the way. Then let the remaining deaerated water of the upper reservoir inject into the specimen again. A total water volume of 10.4 (normalized value in terms of pore volume) has been flowed through the soil specimen. The inlet valve of sedimentation tank should be closed all the way to avoid any possible soil grain loss.

The application of back pressure begins after the completion of the vacuum saturation procedure. In this apparatus, back pressure could be applied from either the double burette or the sedimentation tank (Fig. 2). Both of them are pressurized simultaneously and connected to the tested specimen. Initially the valve connected to the sedimentation tank is closed. The cell pressure and back pressure are increased incrementally with the drainage valves to the double burette, which is connected to the top and bottom of the specimen, opened. The size of each increment is 50kPa. For the majority of tests, a B-value of higher than 0.95 could be achieved after applying a back pressure of 100kPa. At this circumstance, the pressure inside the sedimentation tank reaches 100kPa as well. Then close the double burette valve and slowly open the sedimentation tank valve. Minor adjustments might be necessary to ensure the back pressure reaches 100kPa and then wait until the readings from pressure gauges become stable. The recordings of the load cell inside the sedimentation tank indicate that there is hardly fines loss due to the application of back pressure.

The consolidation is performed by an automatic control system. Cell pressure gradually increases up to the target value at a fairly low increment (i.e., 1kPa/min) to avoid soil grains migration. Axial stress, controlled by a motor, increases correspondingly to keep the determined effective stress ratio (effective axial stress/effective radial stress) constant. In this study, soil specimens are isotropically consolidated until the preferred stress state. After consolidation, the specimens are ready for erosion tests.

4.2 Erosion test

From the erosion test, it is expected to detect the critical Darcy velocity, at which internal erosion initiates. To well demonstrate the mechanical effects of internal erosion on soils, the imposed inflow rate for each specimen should be held constant as a reference. After several trial tests, an inflow rate of 310mL/min for the tested soil is selected because the loss of fines at this rate is significantly large, which would highlight the differences between the eroded specimen (ES) and the non-eroded specimen (NS) in terms of stress-strain relationship. The procedure for the inflow rate increments in this study is shown in Fig. 7. Based on the authors' previous experience of conducting upward seepage tests in a fixed-wall permeameter on the similar sandy soils (Ke and Takahashi, 2012), the initiation of internal erosion would occur at a fairly low Darcy velocity, which is approximately 0.02~0.12cm/s (i.e., equivalent to the inflow rate of 48mL/min~277mL/min through a 70mm-in-diameter circular section) depending on the density and fines content of the tested specimen. Therefore, the initial increment of inflow rate is set approximately at 10(mL/min)/min: increase the inflow rate to 10mL/min in 1min and allow the seepage flow to become steady for the next 1min. The trial tests indicate that a short duration (e.g. 1min) is sufficient to stabilize the seepage flow. As long as erosion initiates, the amounts of eroded fines would increase with the increasing of inflow rate. The increments of inflow rate at this stage could be relatively larger to shorten the test. Then in this study, the inflow rate is increased to the target value of 310mL/min at the increments of 50(mL/min)/min once the it reaches 100mL/min. This inflow rate of 310mL/min will be maintained constant until (1) the recorded hydraulic gradient is steady; (2) the effluent become clear and clean by visual observation; (3) no further eroded fines loss (i.e., <0.2g per 10min); (4) no further increases in the axial and radial strain of the tested specimen. Commonly, the erosion test would be terminated after 3 hours. The inflow rate is decreased gradually till there is no pressure difference between the top and bottom of the specimen. Then close the inflow valve and let the specimen stay still until the readings of the pressure gauges become stable. B-value is checked again.

The stress state of the specimen during the erosion test is maintained the same as that after isotropic consolidation. The cumulative eroded fines mass is recorded automatically by the load cell inside of the sedimentation tank. The balance of the light tray is realized by the following procedure: before the erosion test, the cylinder is filled with deaerated water so that the light tray is fully submerged. After applying the target pressure of 100kPa to the sedimentation tank, the tray would reach equilibrium within 10min. Then set the readings of "eroded soil mass" as zero and start recording. During the erosion tests, authors found that the readings of the cumulative eroded soil mass were influenced by the impact force, generated from the flow jet. It became obvious if larger inflow rate was assigned. To minimize the effect of the impact force on the light tray, a funnel with a 15mm-in-diameter opening at the end has been fastened on the steel frame to surround the inlet pipe. Position of the funnel outlet is aligned with the tray center. The details are shown in Fig. 8. It works as a buffer that could decrease the velocity of flow jet as well as a drainage that could facilitate the eroded fines uniformly settled down onto the light tray. The axial displacement, radial deformation and the pore water pressure difference generated by the seepage flow is recorded at every 1s automatically.

4.3 Undrained and drained compression test

Undrained and drained compression test is performed at the same stress state as that of erosion test to investigate the mechanical consequences of internal erosion. The compression test is displacement controlled with the axial strain rate of 0.1%/min, following the standard criteria (ASTM D4767-11; ASTM D7181-11; JGS 0524-2000; JGS 0525-2000), to allow the pore pressure to reach equilibrium. The confining pressure is maintained constant while axial displacement increases at the designated strain rate. Axial stress could be obtained from the load cell amounted to the piston. The recorded data from the eroded soil collection unit indicate that there is hardly fines loss due to compression.

4.4 Undrained cyclic test

To quantify the effect of internal erosion on the cyclic resistance, undrained cyclic tests are performed on the eroded specimens (ES). After erosion test, the soil specimens are subjected to a cyclic shear stress in axial direction under the same effective confining pressure as that of erosion test with a cyclic stress ratio (CSR) of 0.12. The axial strain rate is 0.5%/min, which is sufficiently slow to allow the equilibrium of pore pressure in the tested specimens.

5 Test Specimens

5.1 Test materials

The grain size distribution of a soil could be split into coarse components and fine components. In this study, the tested specimens are the binary mixtures of two types of silica sands (silica No.3 and No.8) with different dominant grain sizes. The siliceous sand is mainly composed by quartz, categorized as sub-rounded to sub-angular material. According to the Unified Soil Classification System (ASTM D2487), they correspond to SP. The grain size distributions are shown in Fig. 9.

With larger grain size, the silica No.3 sand works as the soil skeleton in the mixtures while the finer silica No.8 sand is the erodible fines. Hereafter, the silica No. 8 is referred to fines for simplicity even though the silica No. 8 is not strictly classified as fines. The mass fraction of silica No.3 and No.8 in the mixture is determined considering the geometrical restriction: the volume of fines should be less than that of the voids among coarse grains. The estimated maximum mass of the fines fraction in the mixture is approximately 37% (Ke and Takahashi, 2012). In this study, a fines content of 35% is adopted. The grain size distribution and the physical properties of the mixture are shown in Fig. 10 and Table 1.

To ensure the internal erosion would occur during the erosion test, the vulnerability of the mixture to internal erosion is assessed by six currently available methods proposed by U.S. Army Corps of Engineers (1953); Istomina (1957); Kezdi (1979); Kenney and Lau (1985, 1986); Burenkova (1993) and Mao (2005). The evaluation results are shown in Table 2. The results indicate that the mixture is potentially unstable and vulnerable to internal erosion if seepage takes place.

5.2 Specimen preparation

The tested specimen is 70mm in diameter and 150mm in height. The technics of moist tamping (Ladd, 1978) is employed to prevent the segregation of the two different sized grains. The method is developed based on the fact that when typical sand is compacted in layers, the compaction of each succeeding layer may further densify the layers below. The concept of "undercompaction, U_n" is recommended to assess the effects of densification. It indicates how much percent a layer should be less densified than the target value. In this study, a non-linear average undercompaction criterion, which is proved to be reliable in generating uniform soil conditions (Jiang *et al.*, 2003), is adopted. The average undercompaction of each layer in a moist tamped specimen is shown in Fig. 11.

The specimen preparation procedures are as follows: determine the oven-dried weights of clean silica No.3 and No.8 for a test according to the fines content and relative density. The initial water content is determined as 10% from the previous trials and errors, at which a uniform specimen would be achieved. Thoroughly mix the soils with deaerated water to make sure the distribution of fines in a specimen is uniform. Equally separate the wet mixture into 10 pieces and keep them in a zipped bag to equalize moisture at least 16 hours before use. The specimen is prepared layer by layer. Weigh the amount of material required for each layer, and place it into the mold by scoop. Each layer is compacted to the required height determined by "undercompaction". The initial soil weight could not be directly checked after preparation. Therefore, the after-test oven-dry weight of the soil specimen together with the eroded soil weight should be checked.

6 Test Results and Discussions

To understand the mechanical effects of internal erosion, several soil specimens are tested. A summary of the test cases is shown in Table 3. The effective confining pressure is 50kPa, which is approximately equal to the earth pressure of 5m in depth. Three different types of triaxial tests, including undrained compression, drained compression and undrained cyclic tests, are conducted on the internally eroded specimens (50EU, 50ED and 50EC). To specify the mechanical consequences of internal erosion, the same triaxial tests are performed on the un-eroded soil specimens (50NU, 50ND and 50NC) at the same effective confining pressure of 50kPa for the comparison purpose.

6.1 Internal erosion characteristics

In this study, hydraulic gradient is defined as the ratio of the recorded pressure drop induced by seepage flow to the specimen length corrected by the vertical deformation. The variation of hydraulic gradient at the initial 900s, 900s~2000s and 0s~11000s during the seepage test is plotted in Figs.12a, 12b and 13a, respectively. Generally, it is indicated that the hydraulic gradient varies with the progress of erosion. For the initial

900s (Fig. 12a), a moderate drop of hydraulic gradient is discovered at 480s (Q=50mL/min, v=0.021cm/s), which is considered as the onset of internal erosion. The effluent becomes slightly turbid with small amounts of fines suspending. However, the eroded soil mass at this stage could not be obtained because the load cell is not able to catch the weight of suspended grains. By visual observation, the suspending fines are very little and therefore, the cumulative eroded soil mass at this stage is considered as zero. A sharp increase of the hydraulic gradient is detected at approximate 880s (Q=100mL/min, v=0.042cm/s) at which the increment of the flow rate begins increasing from 10(mL/min)/min to 50(mL/min)/min (Fig. 12b). The sharp increase may be attributed to the clogging of fines among the constrictions of coarse grains when large amounts of fines begin eroding off. Another possibility is related with the influence of "hammer effects" which refers to the phenomenon that a sudden increase or decrease in flow rate would affect the hydraulic properties of soil specimens (Tomlinson and Vaid, 2000). This effect is obvious when opening the inlet valve at the starting of the tests and closing the valve at the end. It may induce the unexpected movement of soil grains which would affect the detection of critical Darcy velocity. The characteristics of internal erosion are fully exhibited at this stage. The hydraulic gradient dramatically drops while a large amount of fines is eroded off (Fig. 13b), which supposedly results in the increase of effective porosity. If the seepage flow is assumed to follow Darcy's law

($v=ki$), the hydraulic conductivity could be estimated on condition that Darcy velocity and hydraulic gradient is known. It is found that the hydraulic conductivity increases with the decreasing of hydraulic gradient. This trend will continue until a new equilibrium among the soil grains is reached when the hydraulic gradient and the cumulative eroded soil mass become constant. The ultimate hydraulic conductivity is about 150 times larger than the initial value together with the loss of approximately 70% fines (mass ratio of eroded fines to initial fines). No critical clogging is detected at the end of the erosion test probably because the size of voids among coarse grains is sufficiently large for the fines passing through.

The incessant erosion of fines from the tested specimen would lead to a change in the soil fabric, which is represented by the increase of volumetric strain, and void ratio. Figures 13c and d displays the development of the axial and radial strain of the soil specimen during erosion test. In general, the soil specimen is prone to be contractive with the progress of erosion. The soil deformation is found be sudden and rapid. Two obvious jumps in deformation are detected around 2400s and 5600s. It is inferred that along with the dislodgement of the fines, the coarse grains would correspondingly rearrange their relative positions and finally reach a new equilibrium in a short period. This phenomenon is in accordance with the practice. The dam failure induced by internal erosion is usually sudden without any pre-warning, such as a large deformation.

The back pressure in the soil specimen during erosion test is plotted in Fig. 13e. Although the pressure slightly deviates from the target value due to the regular opening/closing of the drainage valve of the sedimentation tank, basically the back pressure is maintained constant in the tested soil specimen. The B-value, checked after erosion test, is usually higher than 0.93, which may indicate a relatively high saturation degree.

6.2 Post-erosion grain size grading

Grain size distribution could characterize the geometrical variation of soil specimens due to internal erosion. Kenney and Lau (1985) concluded that fines loss due to erosion could cause the post-erosion distribution curve shift downward from the original curve. The extent of the movement proportionally increases with the amount of fines loss. In this laboratory test, the post-erosion specimen is equally divided into two layers: top layer and bottom layer. The grain size distribution curve of each layer is determined by performing sieving test (ASTM D6913-04; JIS A1204). The soil of each layer has been oven-dried at 110°C for 24h before sieving. Figure14 shows the typical grain size distribution curves of a post-erosion soil specimen. Both of the post-erosion curves for the upper layer and the bottom layer move downward from the original curve, the extent of which is corresponding to the fines loss. It is noted that there is more fines loss in the upper layer.

6.3 Drained test results and discussions

Figure 15 plots the stress ~ strain curves together with the corresponding volumetric strain curves for the drained monotonic compression on the ES and NS specimens. It is noted that the deviator stress of the ES specimen is larger at the same small strain level (within 1%) comparing to that of the NS specimen while that value becomes smaller at the same medium level (approximately 1% ~ 16%). Both of the volumetric strain curves are contractive and the ES specimen has slightly less volumetric deformation. It is inferred that the larger initial stiffness of the ES specimen is caused by the accumulation of fines at the contact points among coarse grains where local reinforcement may be formed in the seepage test. However, this reinforcement may be deteriorated for the subsequent compression, which is corresponding to the medium strain level. With larger void ratio, the ES specimen at the subsequent compression may show smaller deviator stress at the same axial strain. To validate this assumption, microscopic observations of the eroded soil fabric might be necessary. Overall, the drained strength of the ES specimen is basically lower than that of the NS specimen as expected. It is in accordance with findings by Muir Wood *et al.* (2010) who concluded that internal erosion would cause lower soil strength and Chang *et al.* (2011) who experimentally proved that the drained compressive strength would drop after internal erosion.

6.4 Undrained test results

Undrained tests are conducted at an axial strain rate of 0.1%/min under the initial effective confining pressure of 50kPa. Each test lasts for at least 180min, which may be slow enough to guarantee the full equilibrium of pore pressure with a minimum B value of 0.93. The undrained responses of the tested specimens in terms of stress ~ strain curves are presented in Fig. 16. For the undrained compression, the deviator stress of both the ES specimen and NS specimen reach a marked peak at low axial strain, approximately 1%, followed by the strain softening. When the specimens arrive the phase transformation point the soil behavior becomes dilative. This phenomenon is more obvious in the ES specimen. The peak deviator stress of the ES specimen is fairly larger than that of the NS specimen. However, the after-peak undrained deviator stress of the ES specimen becomes smaller at the medium strain level. Xiao and Shwiyhat (2012) speculatively attributed this higher undrained compressive strength of the ES specimen to the loss of saturation degree during erosion test. From authors' point of view, it might be related with the soil fabric change as well. It is universally accepted that the mechanical behavior of granular soils is highly influenced by the orientation and arrangement of soil grain, and the contact between the grains. The fabric of a soil specimen would be greatly changed by erosion progress and local reinforcement might be formed as is discussed in 6.3. Consequently, the undrained peak deviator stress of the ES specimen may become larger in the small axial strain level. An investigation of the new arrangement of soil grains might be necessary for the further study. To this end, a microscopic observation of the eroded soil fabric should be involved.

6.5 Undrained cyclic test results

Figures 17 and 18 show the cyclic behavior of the NS and ES specimens, respectively, under the cyclic stress ratio of 0.12 with the monotonic compression data superimposed. Both of the specimens show non-reversal loading condition: the plastic axial strain develops with cyclic loops. The NS specimen shows flow deformation, which is common in loose sand. The strain would continue developing with the decreasing of mean effective stress. For the ES specimen, initially, its behavior follows the “flow deformation” pattern. However, this trend is inhibited as soon as the specimen loaded sufficiently to initiate dilation with further straining. Vaid and Chern (1985) termed this phenomenon as “limited flow deformation”. Comparing to the NS specimen, the ES specimen would fail after more cyclic loops. Here the cyclic test data are presented to demonstrate that the apparatus is capable of conducting the undrained cyclic tests on the internally eroded specimens. For further detailed explanations of the cyclic behavior of the internally eroded soil, more tests at different cyclic stress ratios might be necessary.

6.6 Discussions on undrained test results

Commonly, soil becomes loose after erosion due to the large amounts of fines loss (Table 3) and therefore, the eroded soil is expected to show contractive tendency at shearing. However, the undrained monotonic and cyclic tests on the eroded specimens in this study indicate a much dilative behavior after erosion, which may be attributed to the mechanical influence of (1) fines content (*FC*) and (2) geometrical properties of coarse grains. Hitherto, the mechanical influence of non-plastic fines on the soil behavior is somewhat contradictory in literature. Some laboratory investigations indicate the presence of non-plastic fines would result in the increasing of sand dilatancy (Pitman *et al.*, 1994; Salgado, *et al.*, 2000; Ni *et al.*, 2004; among others) while some other studies show a contrary tendency (Zlatovic and Ishihara, 1995; Lade and Yamamuro, 1997; Carraro *et al.*, 2009; among others). The influence of the non-plastic fines content, which is the content of silica No.8 in this study, on the soil undrained strength is experimentally investigated by performing undrained monotonic compression tests on the reconstituted soil specimen with three different fines contents

(0%, 15% and 35%). The soil specimens are prepared by the moist tamping method. Since the void ratio of the eroded specimens is much larger than that can be achieved by the moist tamping method, the initial void ratios are set as large as practical, but are smaller than that of the eroded specimens. Figure 19 plots the stress ~ strain curves together with the corresponding stress paths in stress space for the soil specimens at an effective confining pressure of 50kPa. The initial void ratio and fines content before compression are denoted in the figures. It is noted that the soil specimen with 35% fines content shows partial collapsive behavior after reaching the peak deviator stress: with the subsequent compression, the soil continues deforming and reaching a residual strength. In contrast, the specimen with 15% fines content implies a temporary loss of shear strength after initial peak, which is called "quasi-steady state" in literature. With further compression, the soil becomes dilative and gradually gains strength. In terms of the loose soil specimen without any fines content, the soil response is completely dilative. Therefore, for the tested soil in this study, the presence of the fine silica No.8 sand would decrease the soil strength and restrain the soil dilatancy. One of the consequences of internal erosion is the great amounts of fines loss. The eroded soil specimen with less fines content may show dilative response and consequently, gain higher strength comparing to the un-eroded specimen with higher fines content. Furthermore, the coarse soil used in this study, the artificial silica No.3 sand, shows full hardening behavior without any sign of strength reduction after the yield point even at loose condition (i.e., the initial void ratio is 0.84 in Fig. 19). Dilative soil response caused by the mechanical effect of fines content and geometric properties of coarse grains may have surpassed the contractive tendency induced by the increase in the void ratio. Thus, the eroded soil presents dilative tendency.

6.7 Test repeatability

The repeatability of the seepage test is validated by comparing the primary parameters noted in Table 4. The internal erosion generally occurs at the similar Darcy velocity. However, irregular deviation exists in the hydraulic gradient and hydraulic conductivity, which may be attributed to the difference in homogeneity among the reconstituted soil specimens. The volumetric strain and the cumulative fines loss are basically close, which might imply the good repeatability of the seepage test. In terms of the triaxial tests, the undrained responses of specimen 50EU and 50EU-R are plotted in Fig. 20 to show the consistency of the test data. There are somewhat variations in the undrained response, especially for the post-peak stage. The peak and post-peak deviator stress of the specimen 50EU-R is higher than that of 50EU, which might be due to the difference in the initial void ratio and fines content before the compression test. In contrast, at the initial stage of the compression, both specimens show similar behavior.

7 Summary and Conclusions

A newly developed triaxial internal erosion apparatus, capable of directly investigating not only the hydraulic characteristics of soils at the onset and the progress of internal erosion under preferred stress state but also the mechanical behaviors of those internally eroded soils, is presented. By introducing a sedimentation tank, back pressure could be maintained in the tested specimens during erosion test to ensure a relatively high saturation degree. A measurement system of the cumulative eroded soil mass is installed in the tank to continuously record the eroded soil mass. Erosion tests are performed by constant-flow-rate control manner with the measurement of the induced pressure difference between the top and bottom of the tested specimens. Volumetric strain of the soil specimen could be assessed by measuring the axial and radial deformation. The mechanical consequences of internal erosion could be evaluated by directly performing undrained and drained compression tests or undrained cyclic tests on the eroded soil.

In this study, the binary mixtures of two types of silica sands (silica No.3 and No.8) with different dominant grain sizes are tested. With larger grain size, the silica No.3 works as the soil skeleton in the mixture while the finer silica No.8 is the erodible fines.

For the erosion test, the hydraulic gradient dramatically drops with the erosion of a large amount of fines. The soil grains correspondingly rearrange their relative positions until a new equilibrium is reached. At the end of erosion, the hydraulic gradient and the cumulative eroded soil mass become constant. The ultimate hydraulic conductivity is about 150 times larger than the initial value together with the approximate 70% fines loss (mass ratio of eroded fines to initial fines). The erosion of fines would lead to an increase of the volumetric strain of the tested specimen. The soil deforms in a contractive way. The post-erosion grain size distribution analysis indicates that there is more fines loss in the upper layer.

The drained compressive strength of the ES specimen is lower than that of the NS specimen. For the undrained test, the peak deviator stress of the ES specimen is fairly higher than that of the NS specimen. However, the after-peak undrained deviator stress of the ES specimen becomes smaller at the medium strain level. In terms of the undrained cyclic test, the NS specimen follows the “flow deformation” pattern while the ES specimen shows “limited flow deformation”. The ES specimen would fail after more cyclic loops. Microscopic observations of the eroded soil fabric (i.e., the accumulation spots of fines) might be necessary for explaining the mechanical behavior of the eroded soil.

ACKNOWLEDGEMENT

The first author acknowledges the Japanese Government (Monbukagakusho: MEXT) scholarship support for performing this research. This work was supported by JSPS KAKENHI Grant Numbers 23760440 and 25420498.

NOTATION

e: Void ratio

FC: Fines content

i: Hydraulic gradient

k: Hydraulic conductivity (cm/s)

p': Mean effective stress (kPa)

q: Deviatoric stress (kPa)

Q: Inflow rate (mL/min)

v: Darcy velocity (cm/s)

REFERENCES

Arulanandan, K. and Perry, E.B. (1983), Erosion in relation to filter design criteria in earth dams, Journal of the Geotechnical Engineering Division, American Society of Civil Engineers, Vol.109, No.GT5, 682~698

ASTM D2487, Standard Practice for Classification of Soils for Engineering Purposes (Unified Soil Classification System), Annual Book of ASTM Standards, Vol.04.08, ASTM International, West Conshohocken

ASTM D4221-11, Standard Test Method for Dispersive Characteristics of Clay Soil by Double Hydrometer, Annual Book of ASTM Standards, Vol.04.08, ASTM International, West Conshohocken

ASTM D4647/D4647M-13, Standard Test Methods for Identification and Classification of Dispersive Clay Soils by the Pinhole Test, Annual Book of ASTM Standards, Vol.04.08, ASTM International, West Conshohocken

ASTM D4767-11, Standard Test Method for Consolidated Undrained Triaxial Compression Test for Cohesive Soils, Annual Book of ASTM Standards, Vol.04.08, ASTM International, West Conshohocken

ASTM D7181-11, Method for Consolidated Drained Triaxial Compression Test for Soils, Annual Book of ASTM Standards, Vol.04.09, ASTM International, West Conshohocken

ASTM D6913-04, Standard Test Methods for Particle-Size Distribution (Gradation) of Soils Using Sieve Analysis, Annual Book of ASTM Standards, Vol.04.09, ASTM

International, West Conshohocken

Bendahmane, F., Marot, D. and Alexis, A. (2008), Experimental parametric study of suffusion and backward erosion, Journal of Geotechnical and Geoenvironmental Engineering, Vol.134, No.1, 57~67

Bonelli, S., Brivois, O., Borghi, R., and Benahmed, N. (2006), On the modelling of piping erosion, Comptes Rendus Mécanique, Vol.344, Issues.8~9, 555~559

Briaud, J.L., Ting, F. C. K., Chen, H. C., Cao, Y., Han, S. W. and Kwak, K. W. (2001), Erosion function apparatus for scour rate predictions, Journal of Geotechnical and Geoenvironmental Engineering, Vol.127, No.2, 105~113

Burenkova, V.V. (1993), Assessment of suffusion in non-cohesive and graded soils. Filters in Geotechnical and Hydraulic Engineering, Brauns, Heibaum & Schuler, Balkema, Rotterdam, 357~360

Carraro, J.A.H., Prezzi, M. and Salgado, R. (2009), Shear strength and stiffness of sands containing plastic or nonplastic fines, Journal of Geotechnical and Geoenvironmental Engineering, Vol.135, No.9, 1167~1178

Chang, D.S. and Zhang, L.M. (2011), A stress-controlled erosion apparatus for studying internal erosion in soils, Geotechnical Testing Journal, Vol.34, No.6, 579~589

Chang D.S., and Zhang, L.M. (2013), Critical hydraulic gradients of internal erosion under complex stress states, Journal of Geotechnical and Geoenvironmental

Engineering, Vol.139, No.9, 1454~1467

Decker, R.S. and Dunnigan, L.P. (1977), Development and use of the soil conservation service dispersion test, Dispersive clays, related piping, and erosion in geotechnical projects: a symposium presented at the seventy-ninth annual meeting, ASTM, Chicago, Ill., 27th June~2nd July 1976, Sherard, J.L. and Decker, R.S., Eds., ASTM International, West Conshohocken, PA, 94~109

Haghighi, I., Chevalier, C., Duc, M., Guédon, S. and Reiffsteck, P. (2013), Improvement of Hole Erosion Test and results on reference soils, Journal of Geotechnical and Geoenvironmental Engineering, Vol.139, No.2, 330~339

Indraratna, B., Athukorala, R. and Vinod, J. (2013), Estimating the rate of erosion of a silty sand treated with lignosulfonate, Journal of Geotechnical and Geoenvironmental Engineering, Vol.139, No.5, 701~714

Istomina, V.S. (1957), Filtration stability of soils, Gostroizdat, Moscow, Leningrad

JGS 0524-2000, Method for Consolidated-Drained Triaxial Compression Test on Soils, Standards of Japanese Geotechnical Society for Laboratory Shear Test, Japanese Geotechnical Society, 23~27

JGS 0525-2000, Method for K_0 Consolidated-Undrained Triaxial Compression Test on Soils with Pore Water Pressure Measurement, Standards of Japanese Geotechnical Society for Laboratory Shear Test, Japanese Geotechnical Society, 28~34

Jiang, M.J., Konrad, J.M. and Leroueil, S. (2003), An efficient technique for generating homogeneous specimens for DEM studies, Computers and Geotechnics, Vol.30, 579~597

JIS A 1204 (2003), Grain Size Distribution Test, Soil Testing (Fundamentals and Manuals) (3rd edition), Japanese Geotechnical Society, 27~38 (in Japanese)

Kenney, T.C. and Lau, D. (1985), Internal stability of granular filters, Can. Geotech. J. Vol.22, 215~225

Kenney, T.C. and Lau, D. (1986), Internal stability of granular filters: Reply, Can. Geotech. J. Vol.23, 255~258

Kezdi, A. (1979), Soil Physics: Selected Topics (Developments in Geotechnical Engineering), Elsevier Science Ltd.

Ke, L. and Takahashi, A. (2012), Strength reduction of cohesionless soil due to internal erosion induced by one-dimensional upward seepage flow, Soils and Foundations, Vol.52, No.4, 698~711

Kovacs, G. (1981), Seepage hydraulics, Elsevier Scientific Publishing Company, Amsterdam, Netherlands

Kuwano, R., Connolly, T.M. and Jardine, R.J. (2000), Anisotropic stiffness measurements in a stress-path triaxial cell, Geotehcnical Testing Journal, Vol.23, No.2, 141~157

Ladd, R.S. (1978), Preparing test specimens using undercompaction, Geotechnical Testing Journal, Vol.1, No.1, 16~23.

Lade, P.V. and Yamamuro, J.A. (1997), Effects of nonplastic fines on static liquefaction of sands, Canadian Geotechnical Journal, Vol.34, No.6, 918~928

Lafleur, J. (1984), Filter testing of broadly graded cohesionless tills, Can. Geotech. J. Vol.21, 634~643

Mao, C.X. (2005), Study on piping and filters: part 1of piping, Rock and Soil Mechanics, Vol.26, No.2, 209-215 (in Chinese)

Moore, W.L. and Masch, F.D. (1962), Experiments on the scour resistance of cohesive sediments, Journal of geophysical research, Vol.67, No. 4, 1437~1446

Ni, Q., Tan, T.S., Dasari, G.R. and Hight, D.W. (2004), Contribution of fines to the compressive strength of mixed soils, Géotechnique, Vol.54, No.9, 561~569

Pitman, T.D., Robertson, P.K. and Sego, D.C. (1994), Influence of fines on the collapse of loose sands, Can. Geotech. J., Vol.31, No.5, 728~739

Richards, K.S. and Reddy, K.R. (2007), Critical appraisal of piping phenomena in earth dams, Bull. Eng. Geol. Environ., Vol.66, 381~402

Richards, K.S. and Reddy, K.R. (2010), True triaxial piping test apparatus for evaluation of piping potential in earth structures, Geotechnical Testing Journal, Vol.33, No.1, 83~95

Salgado, R., Bandini, P. and Karim, A. (2000), Shear strength and stiffness of silty sand, Journal of Geotechnical and Geoenvironmental Engineering, Vol.126, No.5, 451~462

Sherard, J.L., Dunnigan, L.P., Decker, R.S. and Steele, E.F. (1976), Pinhole test for identifying dispersive soils, Journal of the Geotechnical Engineering Division, Proceedings of the American Society of Civil Engineers, Vol.102, No.GT1 11846, 69~85

Shwiyhat, N. and Xiao, M. (2010), Effect of suffusion on mechanical characteristics of sand, Proceedings of the fifth international conference on scour and erosion, Burns, S.E., Bhatia, S.K., Avila, C.M.C. and Hunt, B.E., Eds., San Francisco, California, USA, American Society of Civil Engineers, 378~386

Skempton, A.W. and Brogan, J.M. (1994), Experiments on piping in sandy gravels, Géotechnique, Vol.44, No.3, 449~460

Sterpi, D. (2003), Effects of the erosion and transport of fine particles due to seepage flow, International Journal of Geomechanics, Vol.3, No.1, 111~122

Tanaka, T. and Toyokuni, E. (1991), Seepage-failure experiments on multi-layered sand columns-Effects of flow conditions and residual effective stress on seepage-failure phenomena-, Soils and Foundations, Vol.31, No.4, 13~36

Tomlinson, S.S. and Vaid, Y.P. (2000), Seepage forces and confining pressure effects on piping erosion, Can. Geotech. J. Vol.37, 1~13

U.S. Army Corps of Engineers (1953), Filter experiments and design criteria. Technical Memorandum No. 3-360, Waterways Experiment Station, Vicksburg

Uno, T. (2009), The state of the knowledge on seepage failure phenomena, Geotechnical Engineering Magazine, The Japanese Geotechnical Society, Vol.57, No.9, 1~5. (in Japanese)

Vaid, Y.P. and Chern, J.C. (1985), Cyclic and monotonic undrained response of saturated sands, Proceedings of Advances in the Art of Testing Soils Under Cyclic Conditions, Khosla, V., Eds., ASCE, 120~147

Wan, C.F. (2006), Experimental investigations of piping erosion and suffusion of soils in embankment dams and their foundations, Ph.D. dissertation, School of Civil and Environmental Engineering, The University of New South Wales, Sydney, Australia.

Wan, C.F. and Fell, R. (2004a), Laboratory tests on the rate of piping erosion of soils in embankment dams, Geotechnical Testing Journal, Vol.27, No.3, 295~303

Wan, C.F. and Fell, R. (2004b), Investigation of rate of erosion of soils in embankment dams, Journal of Geotechnical and Geoenvironmental Engineering, Vol.130, No.4, 373~380

Marot, D., Bendahmane, F. and Konrad, J.M. (2011), Multichannel optical sensor to quantify particle stability under seepage flow, Can. Geotech. J., Vol.48, 1772~1787

Muir Wood, D., Maeda, K. and Nukudani, E. (2010): Modeling mechanical consequences of erosion, Géotechnique, Vol.60, No.6, 447~457

Xiao, M. and Shwiyhat, N. (2012), Experiment investigation of the effects of suffusion on physical and geomechanic characteristics of sandy soils, Geotechnical Testing Journal, Vol.53, No.6, 1~11

Zlatovic S. and Ishihara, K. (1995), On the influence of non-plastic fines on residual strength, Proceedings of First International Conference on Earthquake Geotechnical Engineering, IS-TOKYO 95', Ishihara, K., Ed., Balkema, Tokyo, Japan, Vol. 1, 239~244

Table 1 Physical properties of tested soil

Physical Property	Value
Specific Gravity, G_s	2.645
Maximum Void Ratio, $e_{\max}$	0.74
Minimum Void Ratio, $e_{\min}$	0.36
Initial Relative Density, D_r (%)	30
Median particle size D_{50} (mm)[(1)]	1.54
Effective particle size D_{10} (mm)	0.038
Uniformity Coefficient C_u	45.9
Curvature Coefficient C_c	0.59
$(H/F)_{\min}$ [(2)]	0.050
$(D_{15c}/d_{85f})_{\text{gap}}$ [(3)]	7.9
Conditional factor of uniformity, h' [(4)]	1.3
Conditional factor of uniformity, h'' [(5)]	8.5
Grain Description	Subround-Subangular

Note:

(1) D_X denotes the grain size finer than which the soil weight by percentage is *X%.*

(2) F is the weight fraction of the soil finer than size d; H is the weight fraction of the soil in the size ranging from d to $4d$.

(3) A soil could be split into a coarse fraction (c) and a fines fraction (f). D_{15c} is the grain size finer than which the soil weight by percentage is 15% for the coarse fraction; d_{85f} is the grain size finer than which the soil weight by percentage is 85% for the fines fraction.

(4) $h'=D_{90}/D_{60}$

(5) $h''=D_{90}/D_{15}$

Table 2 Assessment of the mixture's vulnerability to internal erosion

The method used to assess internal erosion potential		Stability
Criteria	The mixture is internally stable if	
U.S. Army (1953)	$C_u < 20$	U(1)
Istomina (1957) [Ref. Kovacs (1981)]	$C_u \leq 20$	U
Kezdi (1979)	$(D_{15c}/d_{85f})_{\max} \leq 4$	U
Kenney and Lau (1985, 1986)	$(H/F)_{\min} \geq 1$ $(0 < F < 0.2)$	U
Burenkova (1993)	$0.76 log(h'') + 1 < h' < 1.86 log(h'') + 1$	U
Mao (2005)	$4P_f(1-n) \geq 1$(2)	U

Note:

(1) "U" means Unstable;

(2) P_f is the fines content by weight in soil; n is the porosity.

Table 3 Summary of test conditions

Specimen	Initial void ratio	Void ratio after consolidation	Void ratio after erosion	p' (kPa)	Erosion	Test type	CSR(6)
50NU	0.60	0.56	---	50	N(1)	CU(3)	---
50ND	0.59	0.55	---	50	N	CD(4)	---
50EU	0.60	0.55	0.96	50	Y(2)	CU	---
50EU-R	0.60	0.56	1.00	50	Y	CU	---
50ED	0.59	0.55	0.94	50	Y	CD	---
50NC	0.60	0.56	---	50	N	CC(5)	0.12
50EC	0.60	0.57	1.01	50	Y	CC	0.12

Note:

(1) "N" means no erosion;

(2) "Y" means erosion at the assigned inflow rate of 310mL/min;

(3) "CU" means Consolidated-Undrained test;

(4) "CD" means Consolidated-Drained test;

(5) "CC" means Consolidated-Cyclic test;

(6) "CSR" means Cyclic Stress Ratio.

Table 4 Repeatability of seepage tests

Specimen	Critical Darcy velocity (cm/s)	Maximum Hydraulic gradient	Ultimate hydraulic conductivity (cm/s)	Volumetric strain (%)	Cumulative eroded soil mass (g)
50EU	0.021	11.71	2.8	3.94	250.60
50EU-R	0.018	8.86	2.0	3.14	233.15
50ED	0.020	10.05	1.9	3.36	233.30
50EC	0.018	8.51	2.0	3.76	230.29

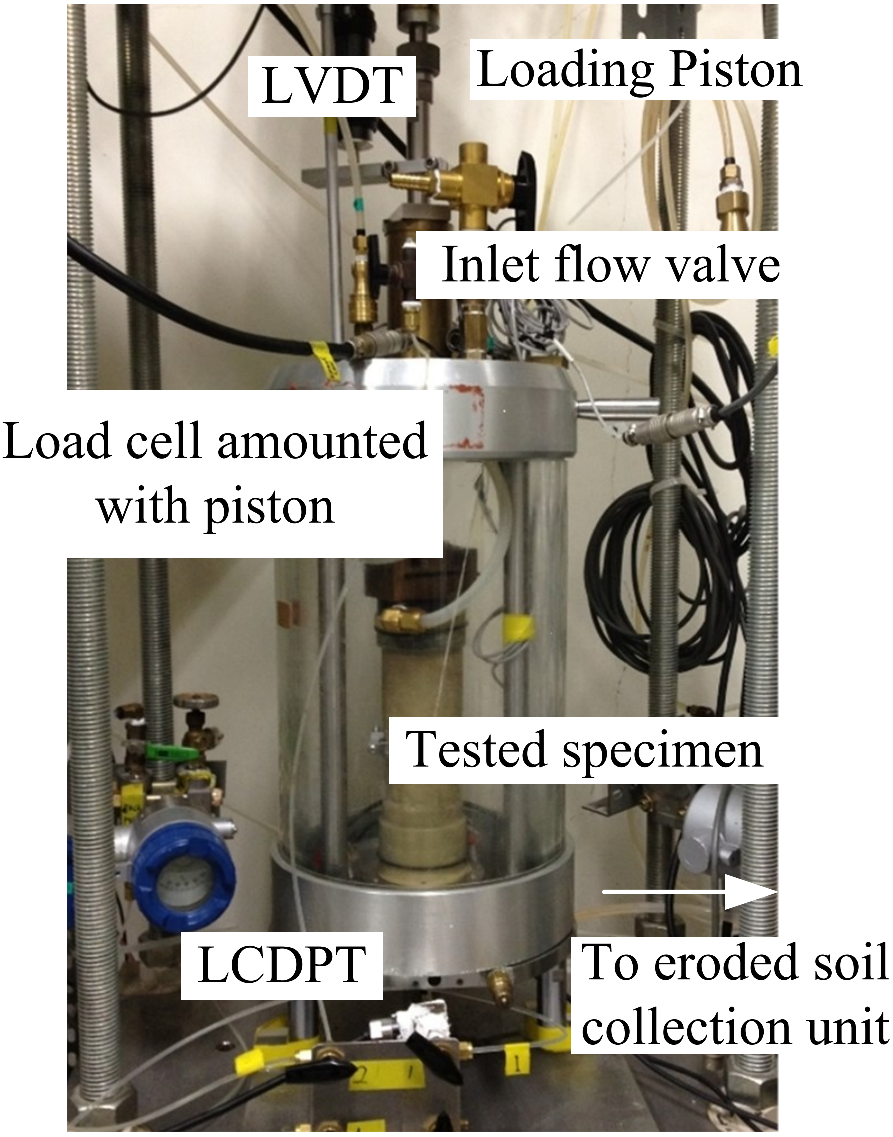

Fig.1 Photography of the triaixial permeameter

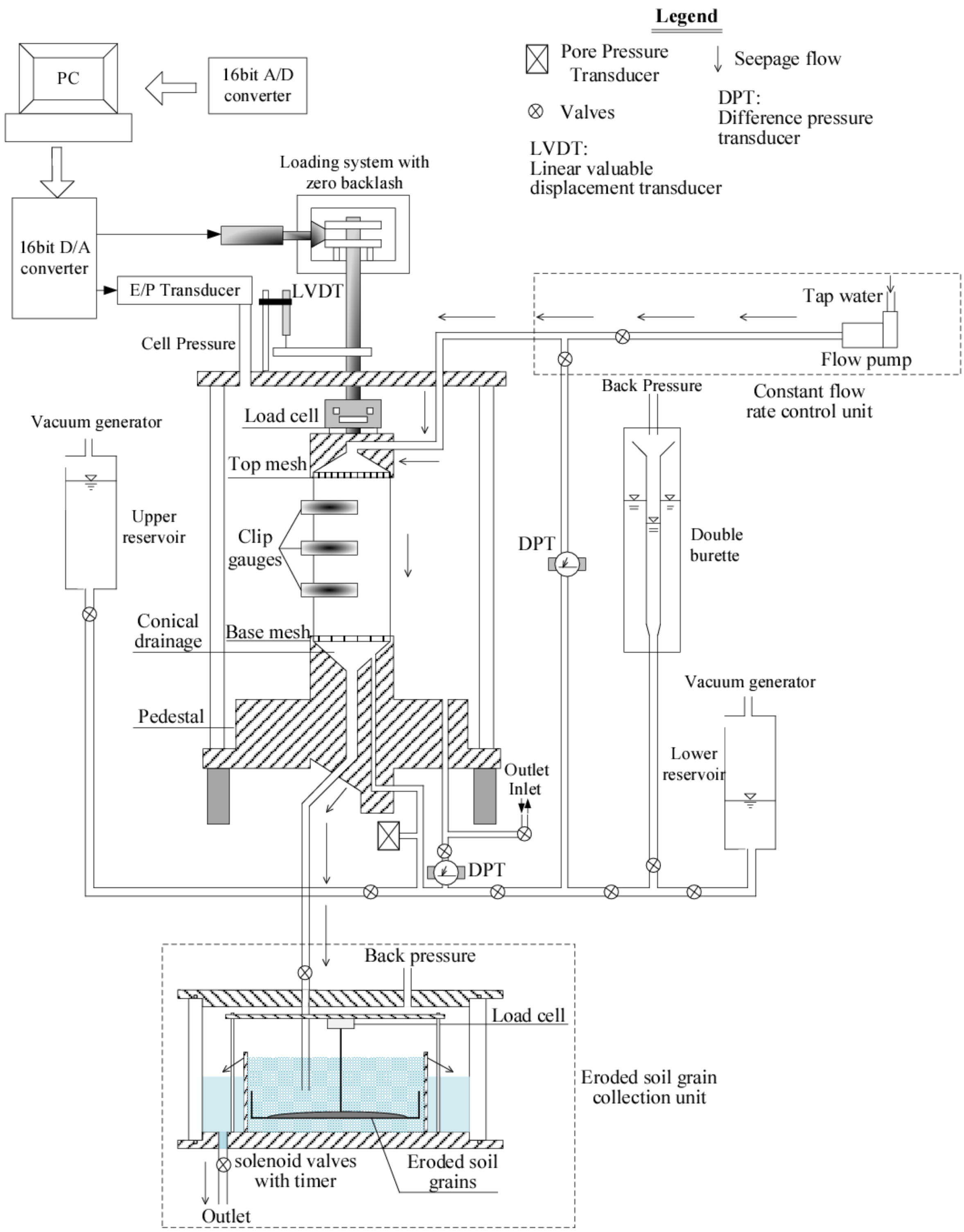

Fig.2 Schematic diagram of main triaxial seepage test assembly

Fig.3 Details of spiral tube

Fig.4 Base pedestal

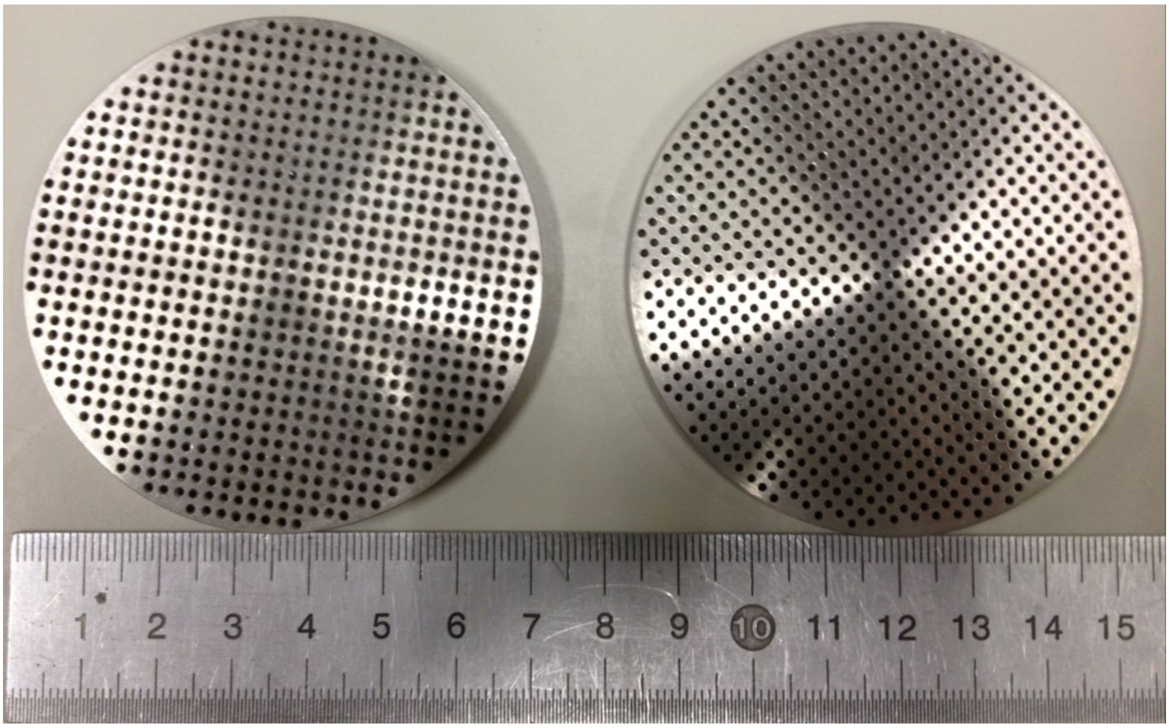

Fig.5 Two 5mm-thick meshes (1mm opening)

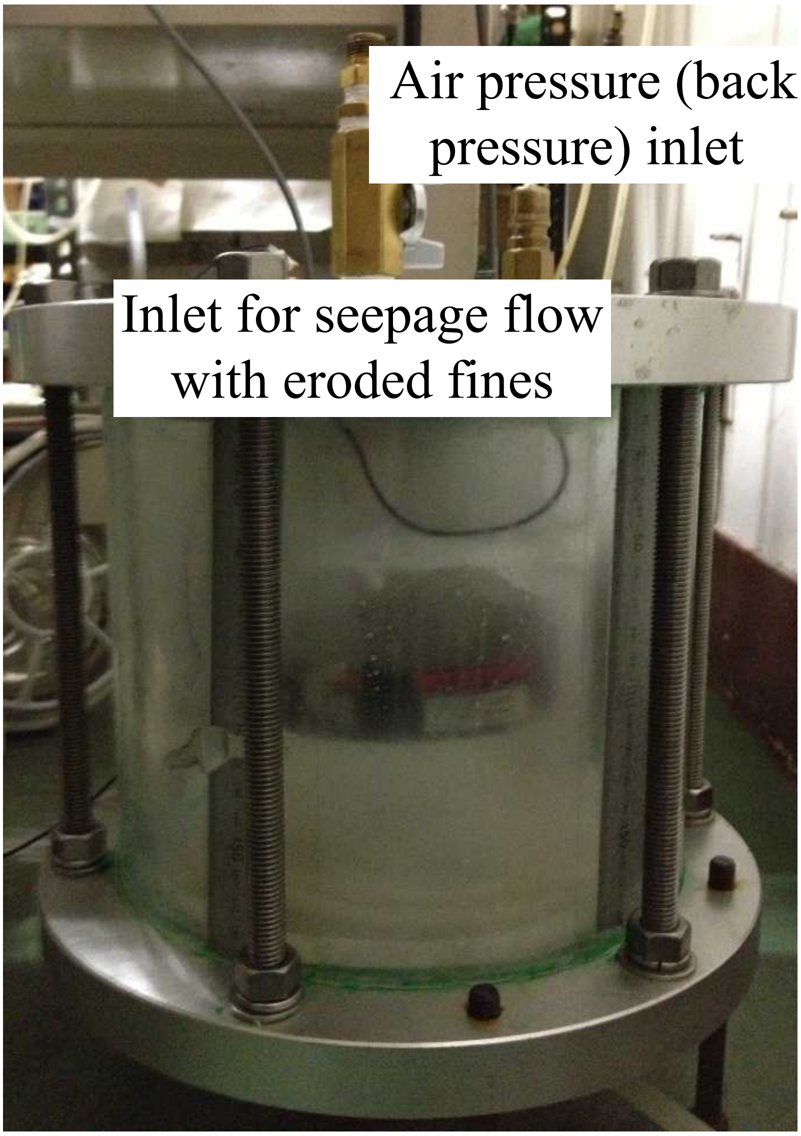

Fig.6 Eroded soil grains collection unit

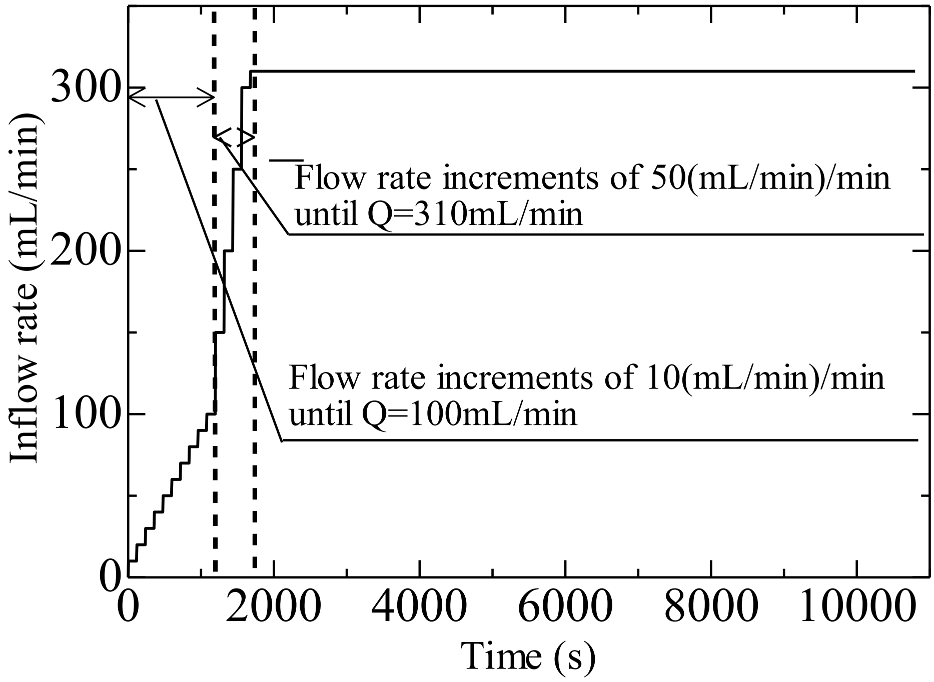

Fig.7 Flow rate increments in seepage test

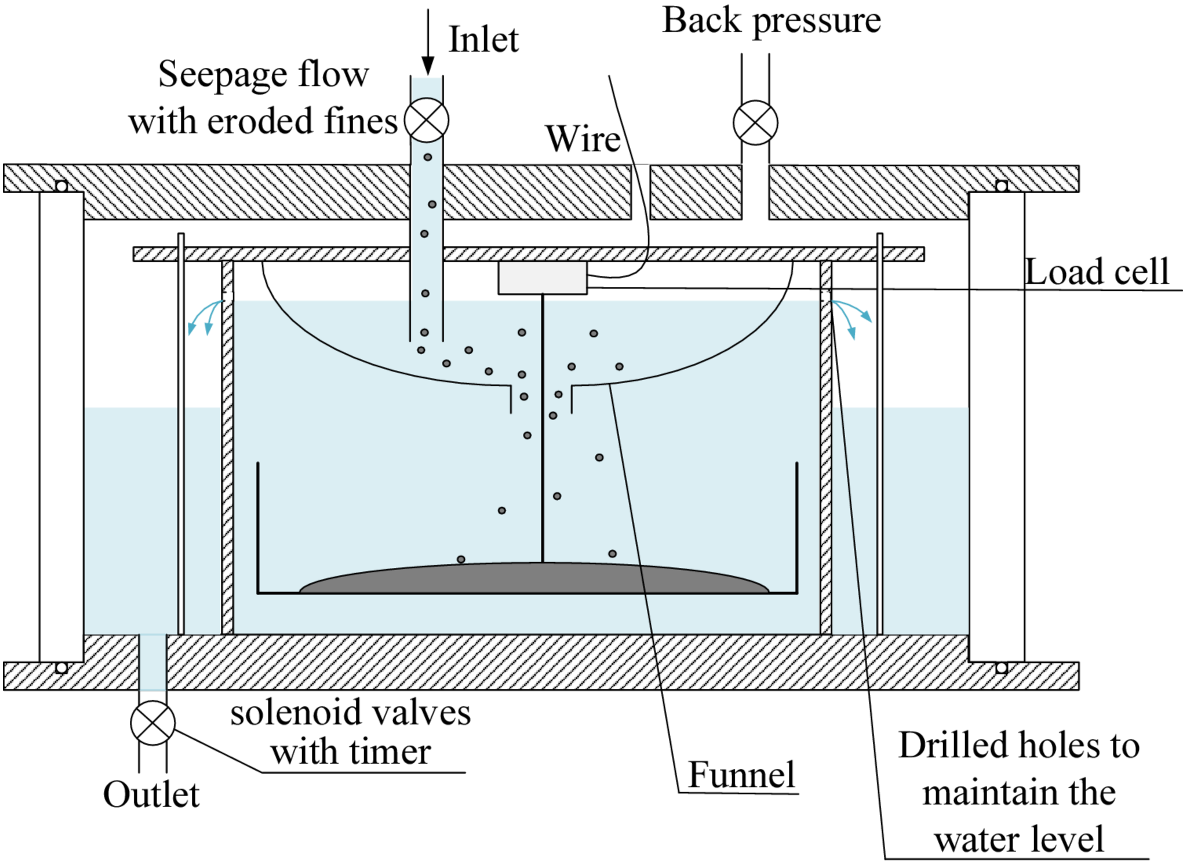

Fig.8 Improved eroded soil particles collection unit

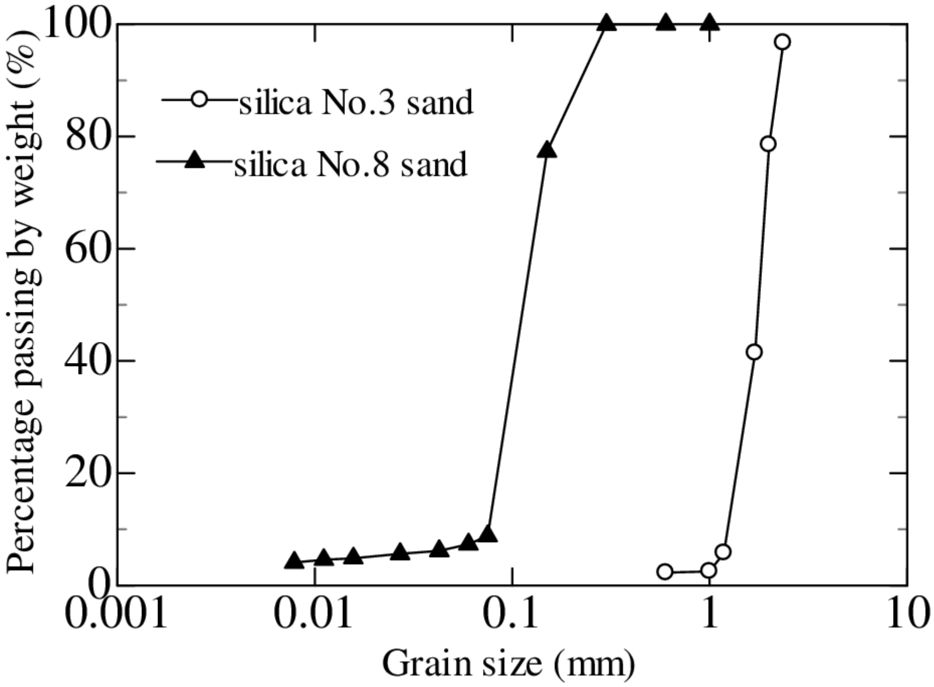

Fig.9 Grain size distribution curves of Silica No.3 and No.8

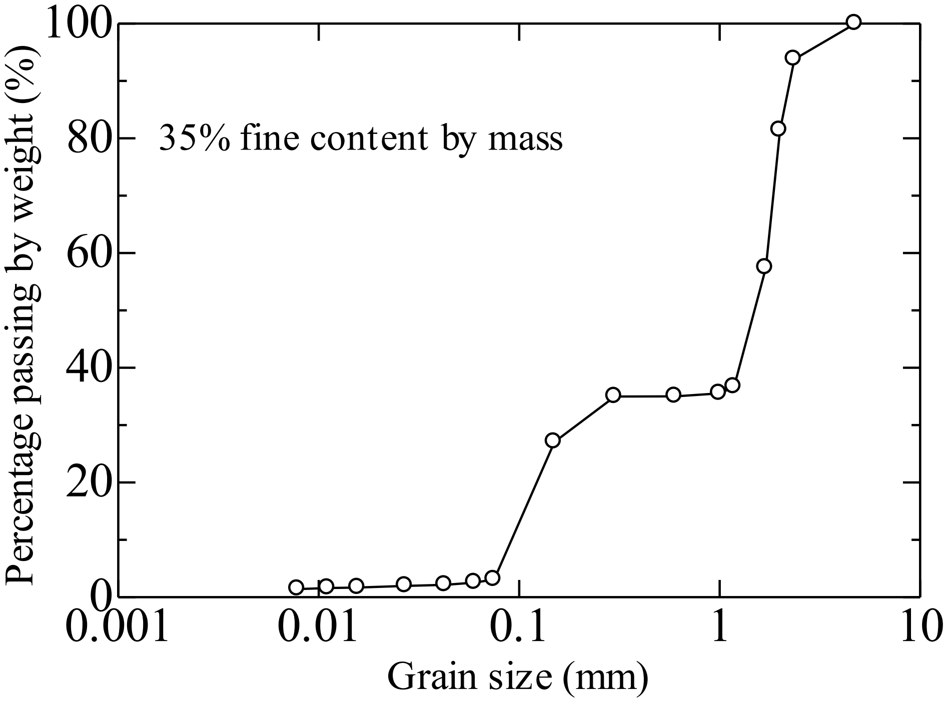

Fig.10 Grain size distribution curve of the mixture

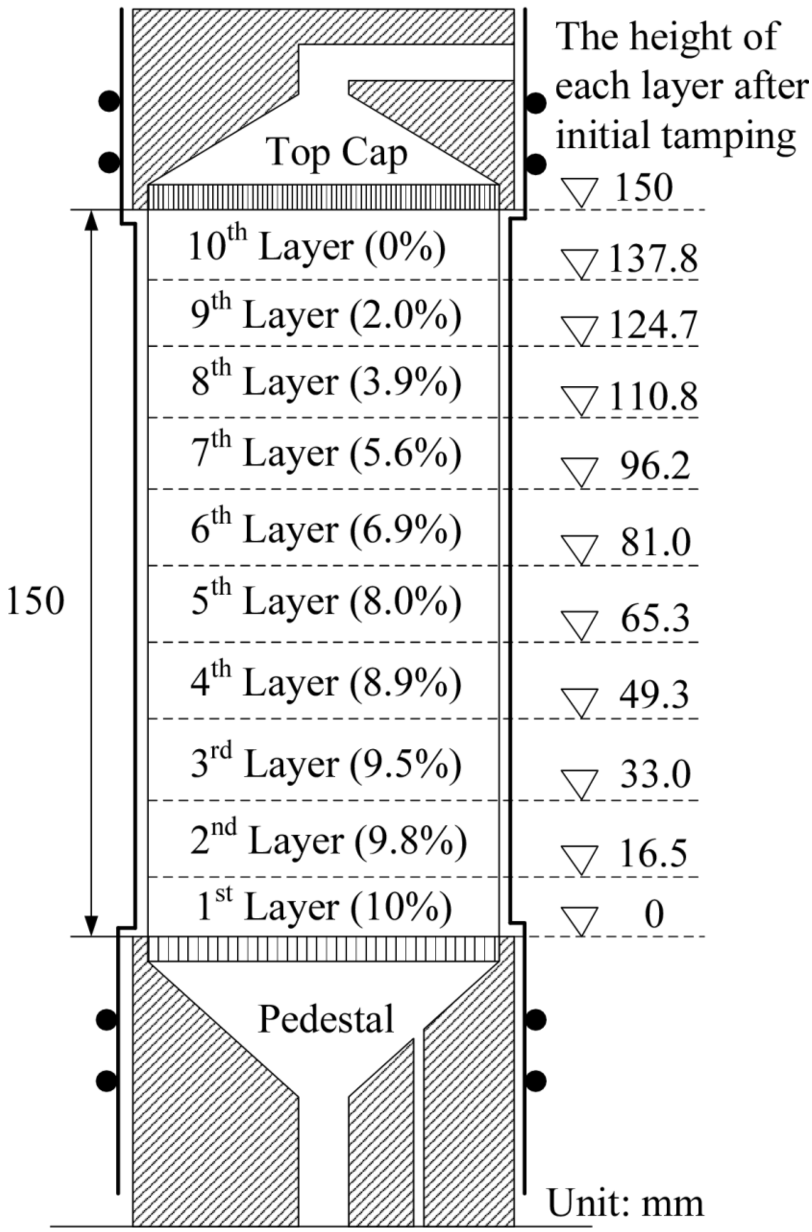

Fig.11 Average Undercompaction of each layer

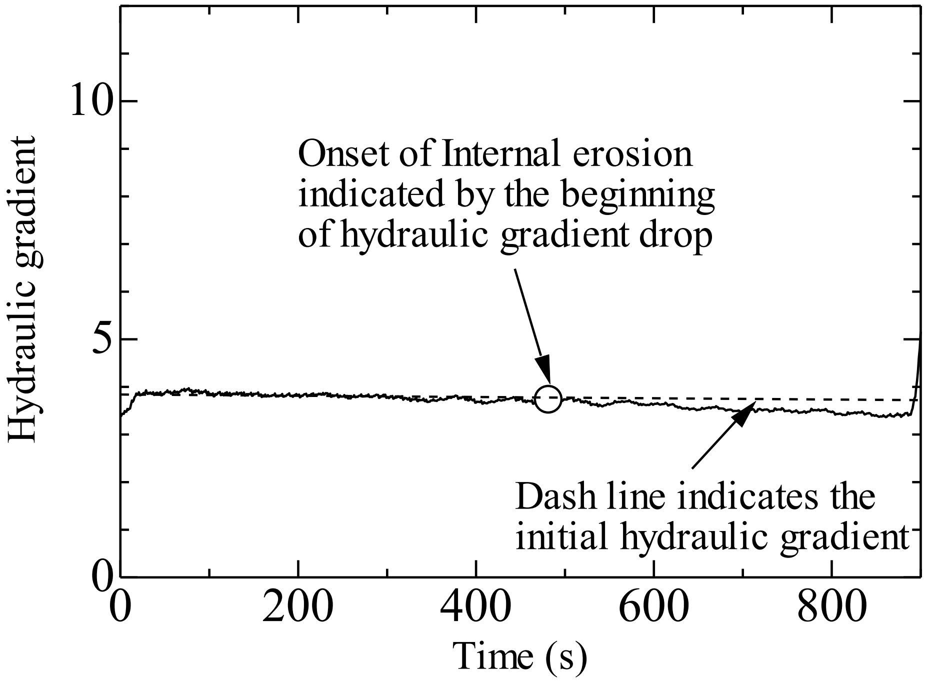

(a) Initial 900s since the beginning of seepage test

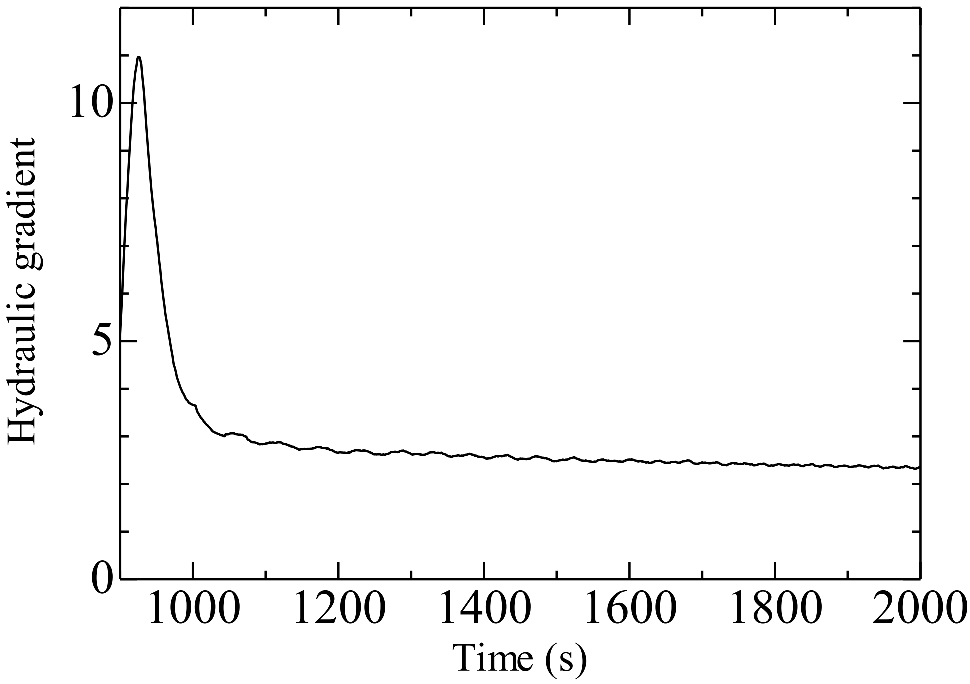

(b) From 900s to 2000s

Fig.12 Change of hydraulic gradient with time (Specimen 50EU)

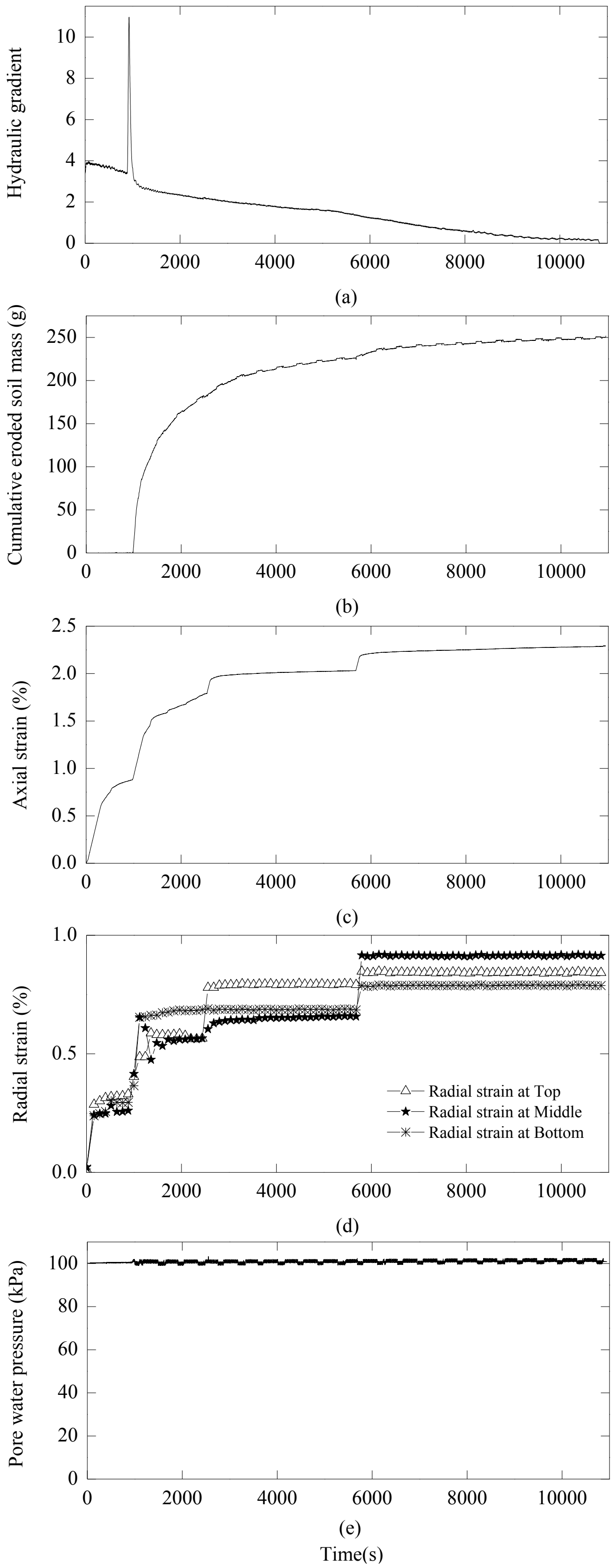

Fig.13 Relation of parameters of seepage tests with time (Specimen 50EU): (a) Hydraulic gradient with time; (b) Cumulative eroded soil mass with time; (c) Axial strain with time; (d) Radial strain with time; (e) Applied back pressure during seepage test.

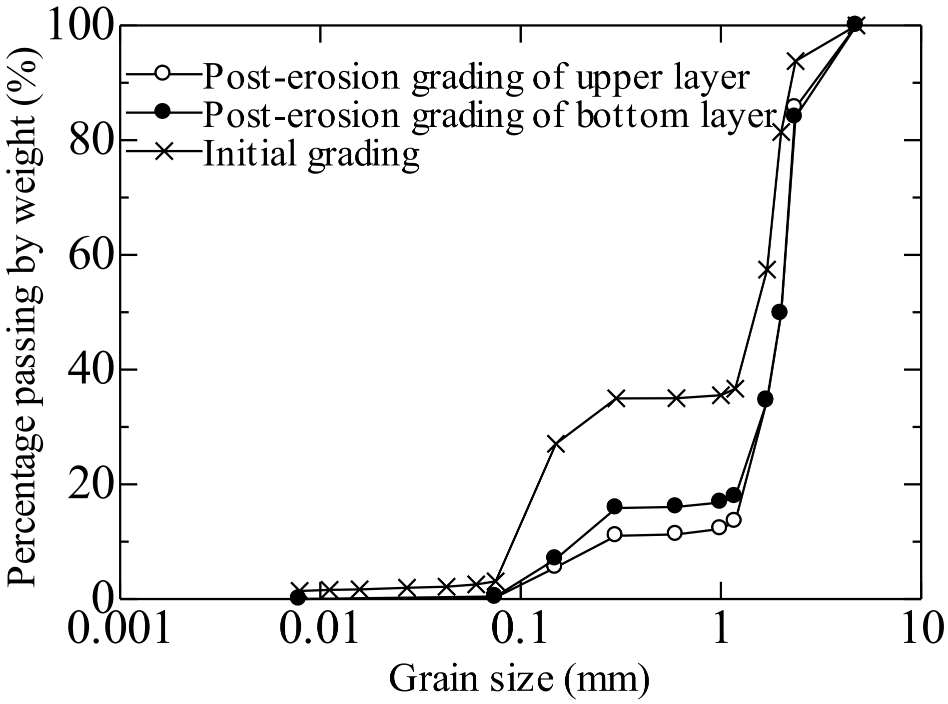

Fig.14 Grain size distributions of the upper and bottom layer of soil specimen after internal erosion (Specimen 50EU)

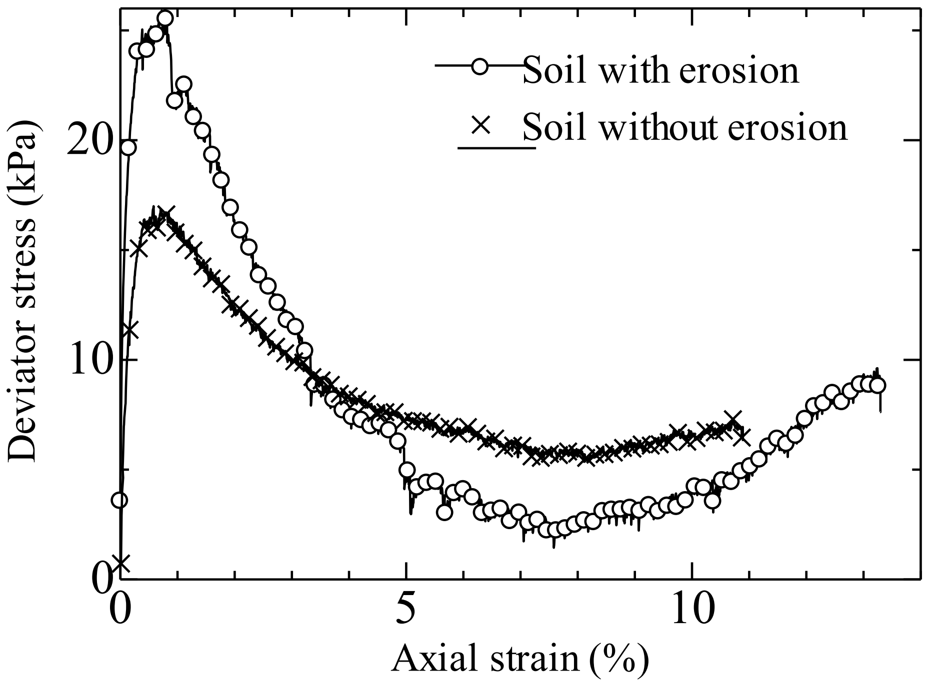

(a) Relation of deviator stress and axial strain

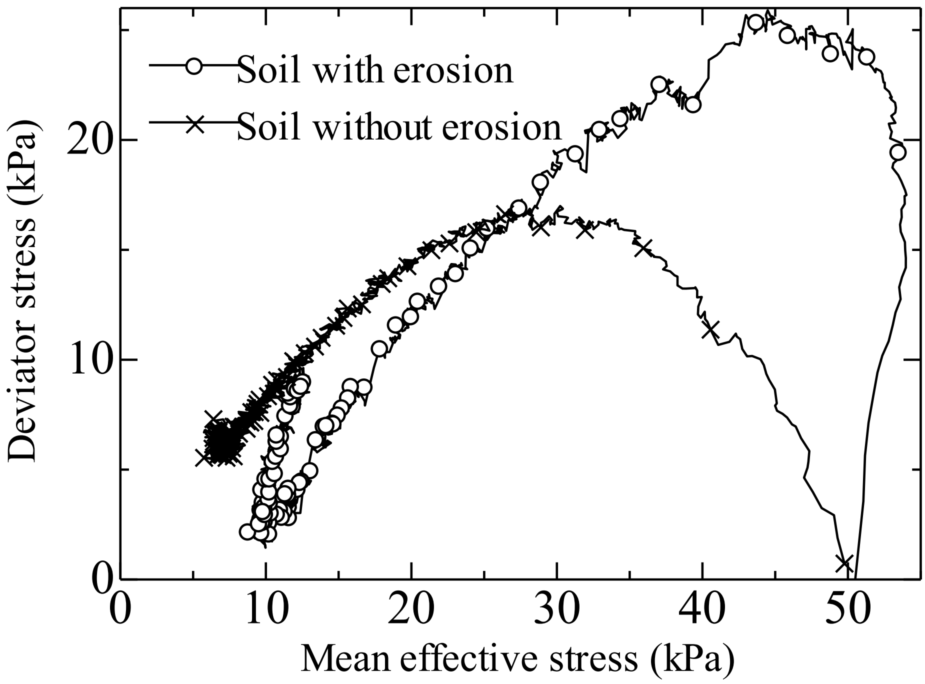

(b) Relation of deviator stress and mean effective stress

Fig.15 Undrained test on the specimens with erosion and without erosion

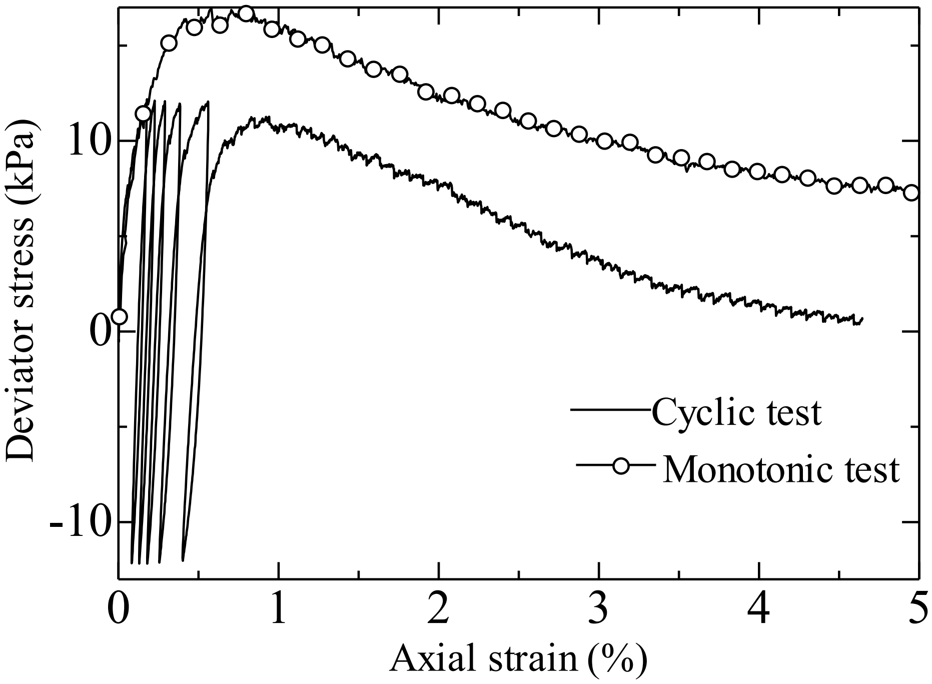

(a) Relation of cyclic deviator stress and axial strain with superimposed monotonic compression test data under undrained condition (CSR=0.12)

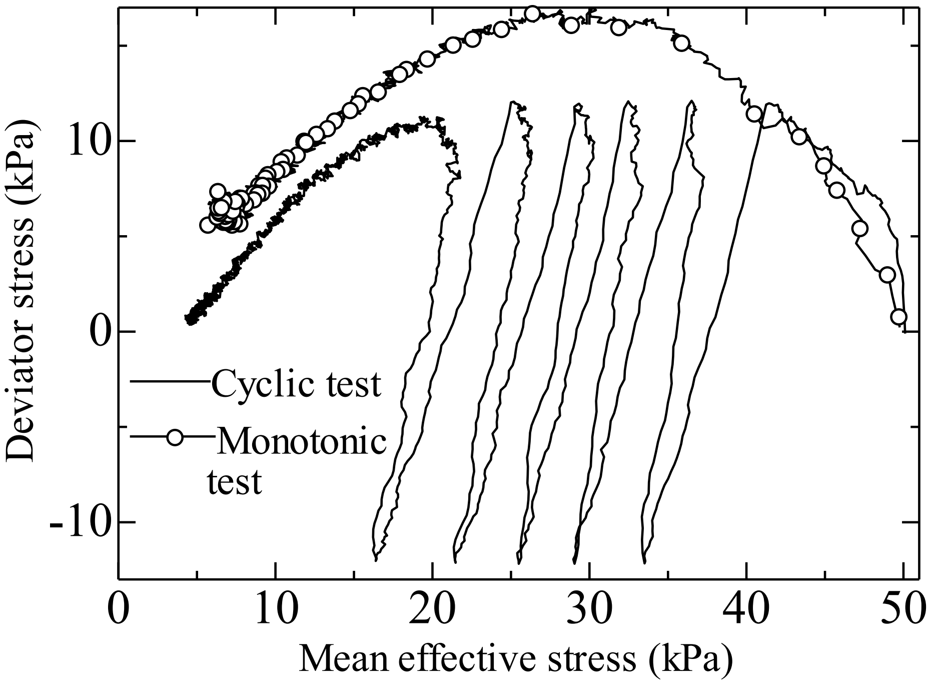

(b) Relation of cyclic deviator stress and mean effective stress with superimposed monotonic compression test data under undrained condition (CSR=0.12)

Fig.16 Cyclic behavior of NS specimen

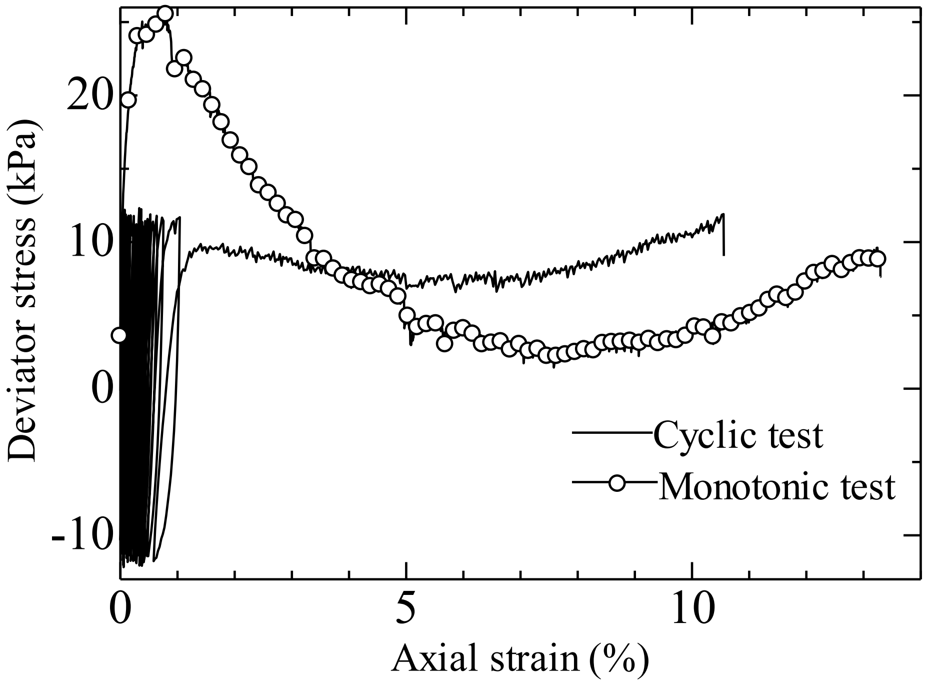

(a) Relation of cyclic deviator stress and axial strain with superimposed monotonic compression test data under undrained condition (CSR=0.12)

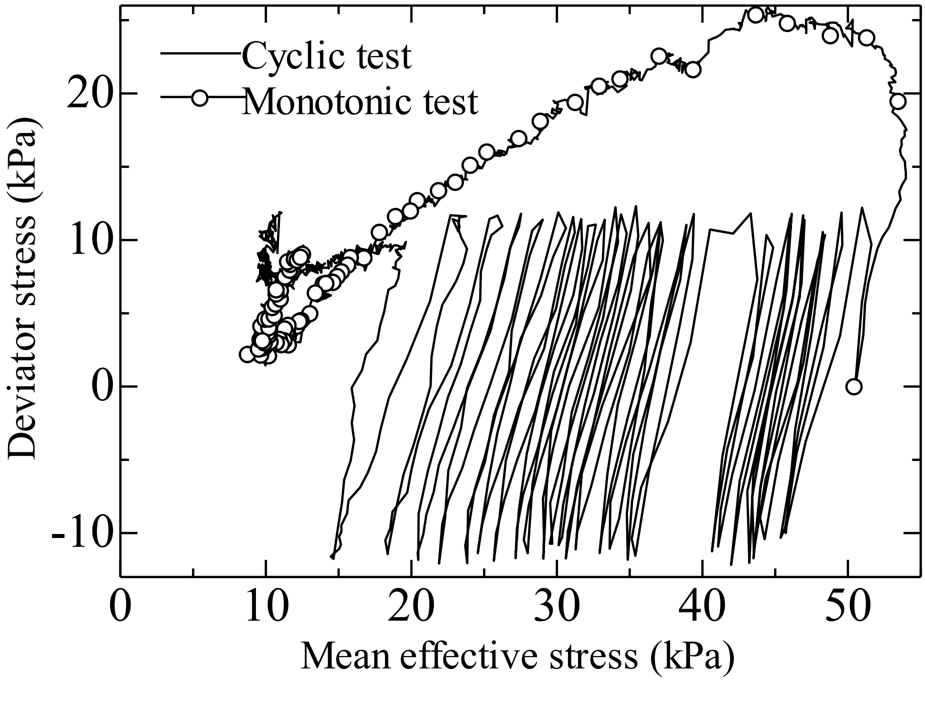

(b) Relation of cyclic deviator stress and mean effective stress with superimposed monotonic compression test data under undrained condition (CSR=0.12)

Fig.17 Cyclic behavior of ES specimen

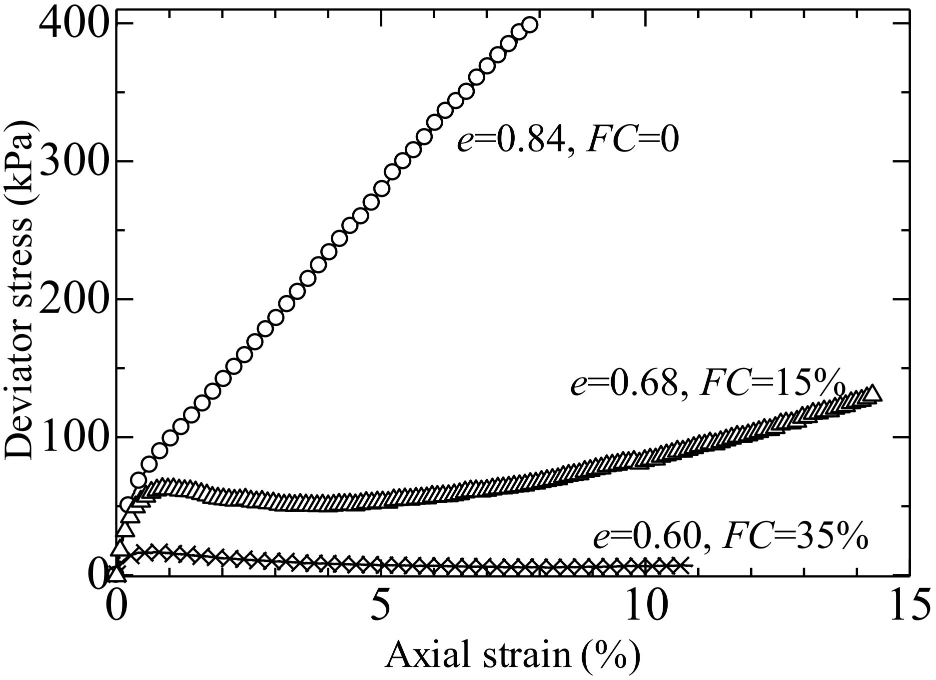

(a) Axial strain versus deviator stress

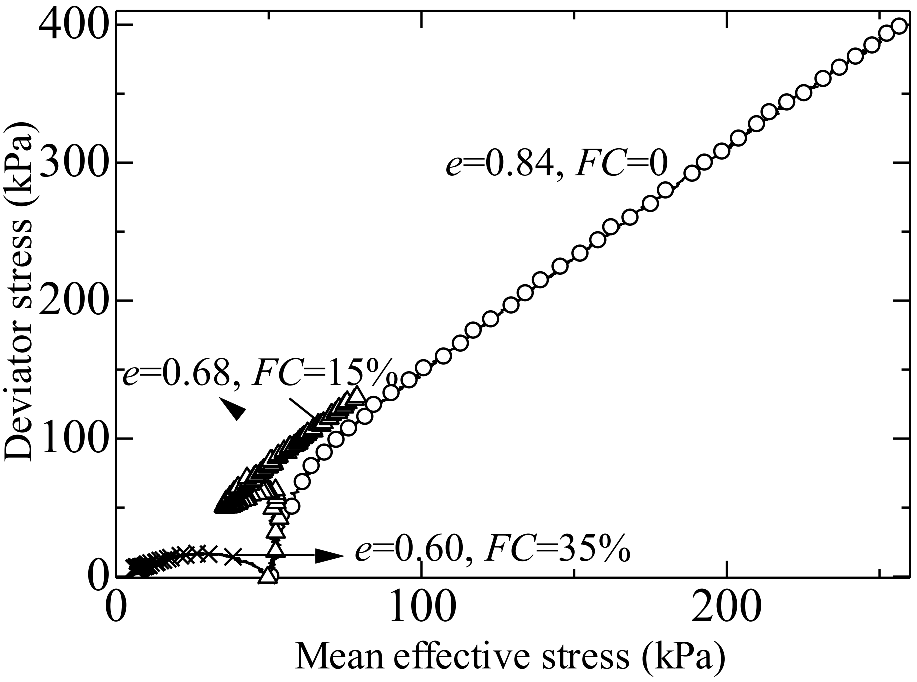

(b) Mean effective stress versus deviator stress

Fig.18 Undrained response of the tested specimens with different fines content

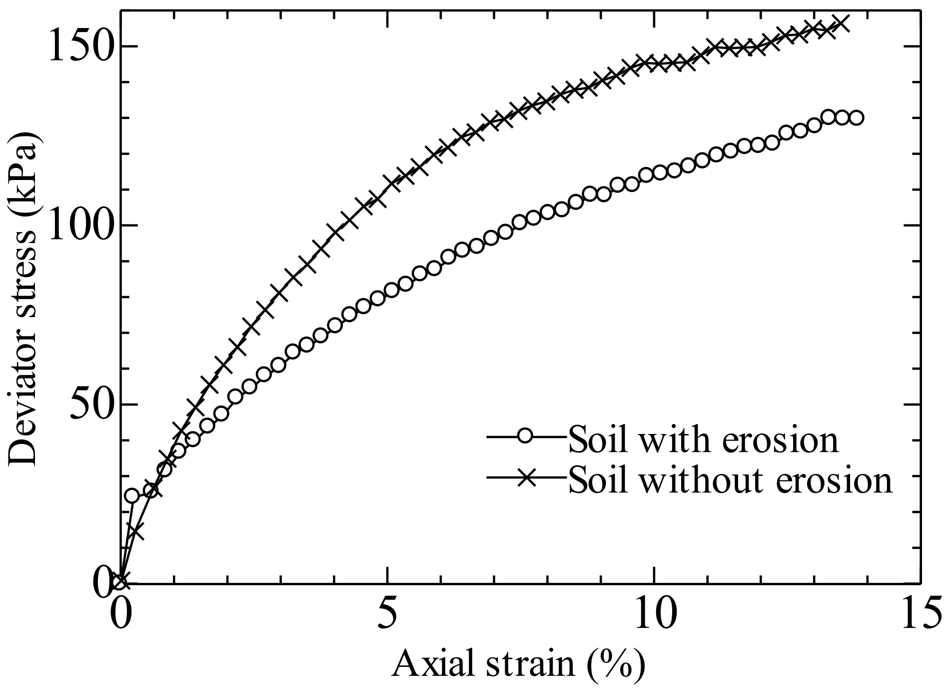

(a) Relation of deviator stress and axial strain

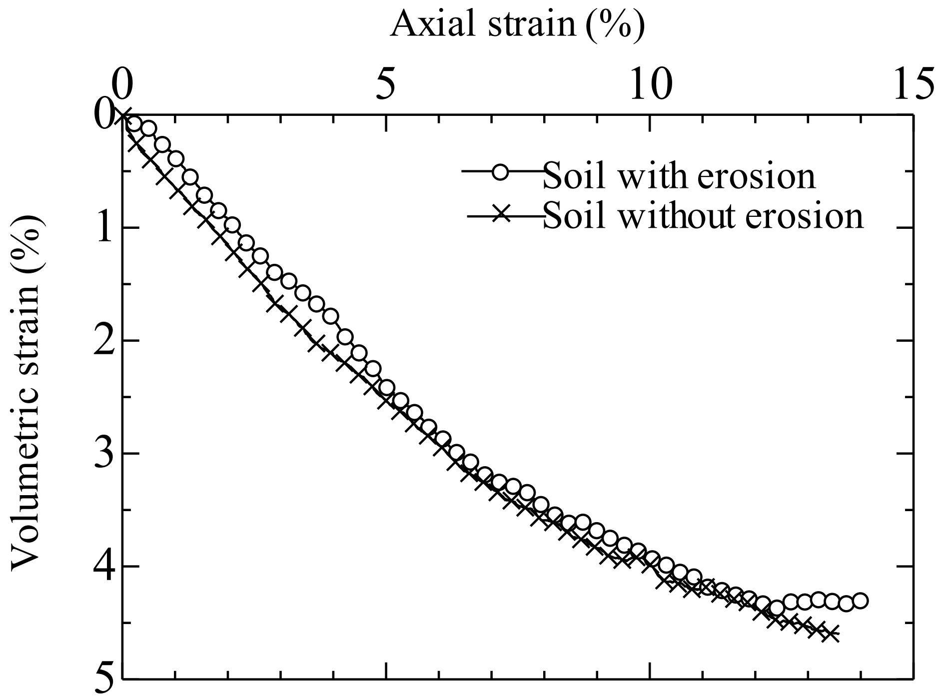

(b) Relation of volumetric strain and axial strain

Fig.19 Drained test on the specimens with erosion and without erosion

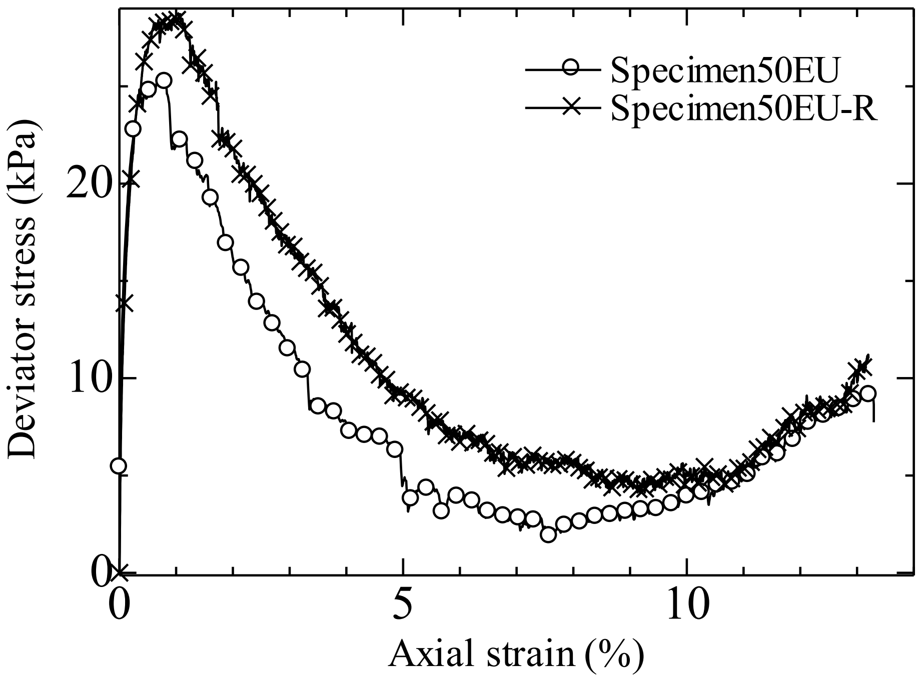

(a) Axial strain versus deviator stress

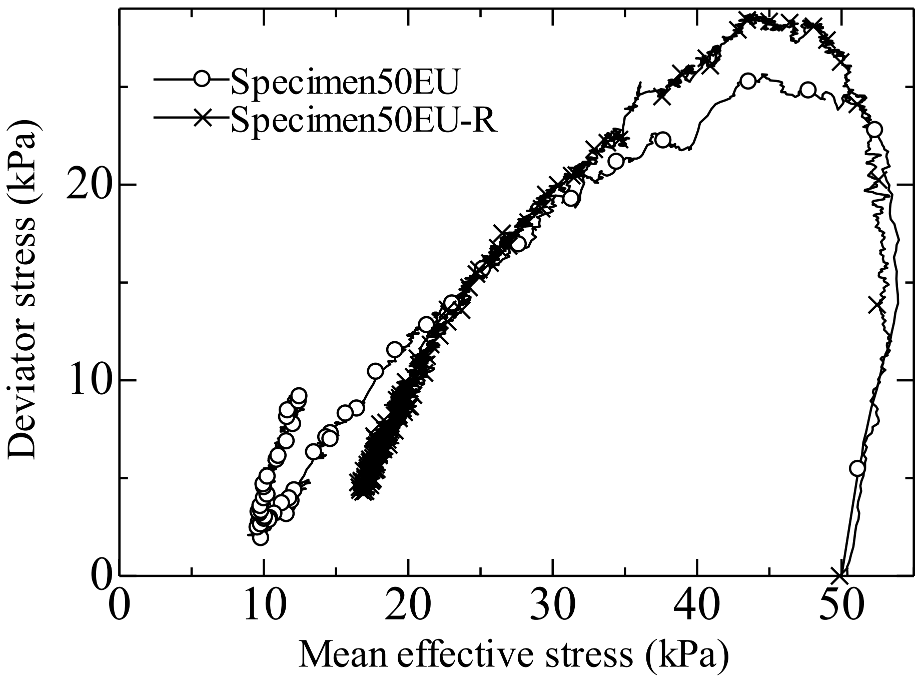

(b) Mean effective stress versus deviator stress

Fig.20 Repeatability of the undrained test on eroded specimen